

Tamara Fletcher
The University of Montana
32 Campus Drive,
Missoula, MT, 59812

April 2019

Dear Prof. Alberto Reyes,

Please find uploaded the revised version of our manuscript, cp-2018-60, "Evidence for fire in the Pliocene Arctic in response to amplified temperature" for resubmission to *Climate of the Past*.

After discussion we have decided that the we are at an impasse with regard to the utility and application of the BRYOCARB and novel empirical model. As a result, we have removed the CO₂ analysis from the revised manuscript while maintaining discussion of our results within the context of the broader CO₂ record for the Pliocene.

Other changes to the manuscript in response to reviewers are detailed below, including clarifying and increasing the explicit discussion of feedbacks in the discussion in response to Dana Royer's suggestions.

We thank the reviewers and yourself for the time invested in this manuscript, and I hope the changes make this manuscript suitable for publication in *Climate of the Past*.

Sincerely,



Tamara Fletcher (On behalf of the authorship team)

Referee #1: Rienk Smittenberg

Although the paper is improved compared to the first submission, I still have major problems with their CO₂ reconstruction. I would agree with their very general observation that higher pCO₂ lead to greater isotope fractionation, however their empirical model has very high - but not well acknowledged - uncertainties rendering it not very useful for a quantitative paleoCO₂ reconstruction

Their basic isotope data are missing from the main text and their calculations are still not fully clear.

They introduce the Bryocarb model but do not give any details on it.

RE: We seem to be at an impasse due to differing opinions on the utility of BRYOCARB and the empirical model as devised for this study. As such, the CO₂ component of this paper has been removed.

The general writing style is still not very good in part, and not built up logically here and there, this should be given a careful look (again).

I have uploaded an annotated pdf with more detailed comments

Comments copied out of the PDF:

Line 138: Strike out (Δ 13 C)

RE: The CO₂ component of this paper has been removed.

Line 141: Farquhar proposed to use Big delta 13C as a term for isotope fractionation effect (or discrimination) and this is still common in the ecosystem isotope literature. However there is a broader consensus of using epsilon for this, reserving Big Delta to express simply the difference between two pools/species. The isotope fractionation factor, again, is expressed by alpha. At the moment the various styles are mixed in the text and this is confusing. The authors need to be consistent in their isotope language.

RE: The CO₂ component of this paper has been removed.

Line 144: Strike out ~~isotopic fractionation~~

RE: The CO₂ component of this paper has been removed.

Line 145 strike out –

RE: The CO₂ component of this paper has been removed.

Line 147: Strike out ~~in~~

RE: The CO₂ component of this paper has been removed.

Line 157: What would be the effect of lowering pO₂ levels, reducing the inhibition of photosynthesis due to photorespiration?

See Dai, Z., Ku, M.S.B. & Edwards, G.E. Planta (1996) 198: 563.

<https://doi.org/10.1007/BF00262643>

RE: The CO₂ component of this paper has been removed.

Line 176: Note there is a 0.2 permil difference between growing season summer CO₂ and mean mean annual.

RE: The CO₂ component of this paper has been removed.

Line 178: explain what 'sub-fossil' entails here.

RE: The CO₂ component of this paper has been removed.

Line 179: reference to BRYOCARB model missing, and it is totally unclear what this model does and why it is used.

RE: The CO₂ component of this paper has been removed.

Line 181: At this point in the text it is fairly unclear what this transfer function entails, one would expect some equation.

RE: The CO₂ component of this paper has been removed.

Line 182: If the Bryocarb model is calibrated with own data then how can it be independent from that?

RE: The CO₂ component of this paper has been removed.

Line 185: sentence is oddly constructed and hard to understand, and I doubt you went back in time to the Pliocene

RE: The CO₂ component of this paper has been removed.

Line 186: simultaneous with what

RE: The CO₂ component of this paper has been removed.

Line 188: Strike out ~~Δ13-C~~ and ~~material~~

RE: The CO₂ component of this paper has been removed.

Line 189: There is a quite a large spread in isotope discrimination among different Tunda types, from 14 to 20 permil, with a very high sensitivity to mean annual temperature, see the figure from Buchman&Kaplan (2001) in Pataki et al (2003) GlobBiogeochemCycles17-1022

RE: The CO₂ component of this paper has been removed.

Line 189: if it is sensitive to altitude, does that not undermine the assumptions used to make the transfer function?

RE: The CO₂ component of this paper has been removed.

Line 192: why not take the ERA interim data?

RE: The CO₂ component of this paper has been removed.

Line 192: I assume one gets one (average) estimate of p(i)/p(a) because we only have one atm. 13C?

RE: The CO₂ component of this paper has been removed.

Line 206: MAAT?

RE: The suggested change has been made.

Line 221: Strike out ~~The~~.

RE: The wording here has been changed.

Line 227: Strike out ~~then~~.

RE: Change made

Line 241: Calculating MST comes out of the blue in the text, needs to be introduced a little earlier

RE: This has been introduced at the end of section 2.3

Line 253: It would be useful to mention the RMSE's of these calibrations, i.e. the uncertainty of the proxy (let alone the uncertainty in the measurements)

RE: This is now provided in equations 3, 4 and 5.

Line 294: There are three stippled lines in Fig 3 one being the Bryocarb relation, this is confusing.

RE: The CO₂ component of this paper has been removed.

Line 302: In my opinion this large spread of sensitivity is highly problematic. On top, they come from hugely different ecosystems with undoubtedly different types of mosses. Essentially the authors have (re)produced four estimates of the sensitivity (S) of fractionation with elevation, and it clearly shows that the various factors like humidity, temperature, but also possibly canopy effect, wind, etc, play into the game. In my opinion it is not warranted to pool all these results and come with one S, instead they should combine the four estimates of S which then has an uncertainty associated with it (also including the uncertainties of the individual S). That said, they come with a prediction interval in Fig. 3 that does have a spread of 7 permil for any given pCO₂. In other words, one needs a 7 permil difference in $\delta^{13}\text{C}$ between fossil mosses arrive at the statement they grew under significantly different pCO₂ levels.

RE: The CO₂ component of this paper has been removed.

Line 307: But we are discussing the modern calibration here?

RE: The CO₂ component of this paper has been removed.

Line 320: An estimate of the error of the slope (and intercept) is missing

RE: The CO₂ component of this paper has been removed.

Line 320: $\delta^{13}\text{C} \times \Delta \delta^{13}\text{C}_{\text{moss}}$?

RE: The CO₂ component of this paper has been removed.

Line 323: add table

RE: The CO₂ component of this paper has been removed.

Line 326: and measured fossil moss $\delta^{13}\text{C}$ values. These values should be shown in the paper!!

RE: The CO₂ component of this paper has been removed.

Line 328: Not clear at all where this 50ppm error comes from. It is different than the range of 296 - 480?

RE: The CO₂ component of this paper has been removed.

Line 328: what is the transfer error?

RE: The CO₂ component of this paper has been removed.

Line 333: That it is not different already shows from figure 3 where the Bryocarb solution falls within the 'empirical' range. The latter model is thus equally imprecise. Another problem

is the calibration range, which goes to 36 Pa (approx 360ppm) thus anything beyond that is an extrapolation - however there is no indication why the relation should be linear.

RE: The CO₂ component of this paper has been removed.

Lines 336-341: Anyone not intricately familiar with the brGDGT literature will be totally confused by these long sentences.

RE: Edits have been made to improve clarity.

Line 360: I'd say the quantification becomes different, not the abundance itself.

RE: This change has been made.

Line 376: If the RMSE of that calibration is +/- 2.5', how can a reconstruction be more precise?

RE: This is the standard deviation, not the RMSE. The text has been edited to reflect this.

Line 450: what is a 'slope of less isotopic discrimination'?

RE: The CO₂ component of this paper has been removed.

Line 460: and slopes

RE: The CO₂ component of this paper has been removed.

Line 469: The above is a good discussion. Concluding there are uncertainties in the approach. The next step is to quantify that uncertainty.

RE: The CO₂ component of this paper has been removed.

Line 475: Strike out ~~highly variable~~

RE: The CO₂ component of this paper has been removed.

Line 480: 0.17 mg/C means??

RE: The CO₂ component of this paper has been removed.

Line 482: which one is that? the one of -20.9 permil?

RE: The CO₂ component of this paper has been removed.

Line 483: Abrupt transition about some other proxies,

RE: The CO₂ component of this paper has been removed.

Line 493: And then suddenly back to own estimates

RE: The CO₂ component of this paper has been removed.

Line 449: But that is only really because the ocean carbonate system cannot keep up at the moment exchanging and buffering the light C from fossil fuels. To sustain a very low ¹³C over a long time scale the geological C cycle needs to look very different. Is there any carbonate ¹³C evidence for low ¹³C?

RE: The CO₂ component of this paper has been removed.

Line 555: Many grammatical errors in this paragraph

RE: The authors have made changes that we hope improve this paragraph

Line 582: Posited by whom?

RE: Change made. We posit that.

Line 602: where do these numbers come from?

RE: The exploratory CRACLE analysis described from 597. We now specify which analysis at that point in the text.

Line 649: Importantly, this is just one site and may not be representative for the entire Pliocene Arctic.

RE: Changes to this section of the text now highlight this point and the need for additional palaeofire studies at other sites in the CAA.

Line 654: add uncertainty

RE: This change has been made.

Referee #2: Dana Royer,

I'll start my review with two core concerns:

1) There is a fundamental disconnect in the manuscript. The Abstract and Introduction set up as a central tenet the link between fire frequency and climate amplification in the Arctic:

Abstract: "One intriguing, but not fully understood, feature of the early to mid-Pliocene climate is the amplified arctic temperature response. Current models underestimate the degree of warming in the Pliocene Arctic and validation of proposed feedbacks is limited by scarce terrestrial records of climate and environment, as well as discrepancies in current CO₂ proxy reconstructions. Here we reconstruct the CO₂, summer temperature and fire regime from a sub-fossil fen-peat deposit";

Introduction: "We propose that fire in arctic ecosystems may also be an important mechanism for amplifying arctic surface temperatures during the Pliocene, and so seek to understand its characteristics through quantification from the sediment record".

But this theme is not returned to; not in the Abstract, and not in the Discussion. This leaves the reader unsatisfied. The authors do not even state whether temperature amplification exists for their site (beyond what is predicted from Pliocene global climate models), despite having the (summer) temperatures and CO₂ concentrations to do so. That would be step 1.

Let's assume that an exaggerated amplification is present (relative to GCMs). The authors have strong evidence for wildfire. Could wildfire amplify the temperature response to an increase in greenhouse gas forcing (relative to the feedbacks present in GCMs currently used for the Pliocene)? Again, the authors do not lay out these arguments.

An alternative approach would be to present the CO₂, temperature, and fire data, and leave it at that, with only some minor comments about climate feedbacks. That is essentially how the manuscript is currently written, if one were to remove the above-mentioned sections in the Abstract and Introduction. That would be a fine paper.

RE: The authors consider that this theme was returned to in the discussion, both implicitly through discussion of the feedbacks between fire and temperature, fire and climate, vegetation and climate, and vegetation and fire, and explicitly 970–976 (current markup

manuscript line numbers). This section references the preliminary work conducted on wildfire as a feedback due to its “complex direct impacts on the surface radiative budget and direct and indirect effects on the top of the atmosphere radiative budget (Feng et al., 2016).”

The conclusion linked the interactions between climate, CO₂, vegetation and fire. It also explicitly states the need for modelling experiments to “quantitatively investigate the effects [on climate] of the kind of fire regime presented here”.

To make the link to feedbacks clearer, have now changed the title of the manuscript, the discussion subheading, added short sections within the discussion that highlight the nature of these relationships as feedbacks, and added more details of the kinds of direct impacts we might expect in the final paragraph of the discussion. We have also devised a new figure that demonstrates the feedbacks between fire, vegetation and temperature in this ecosystem. This aspect has also been de-emphasised in the introduction through the removal of some background material.

2) Given the first set of reviews, I’m surprised that the authors continue to emphasize their empirical CO₂ model. The fact that the BRYOCARB slope is shallower than the empirical one (Figure 3) should concern them. As the authors mention in the main text, there’s something funky going on with the Poland data. Those data steepen the empirical slope. As the authors also mention in the main text, the Andes data, which span the most elevation and perhaps have the least variability in other environmental factors (like moisture), show a shallower slope that looks close to the BRYOCARB slope. So why emphasize the empirical equation?? Especially because it requires extrapolation beyond the calibration data (which the authors do not acknowledge).

The errors with BRYOCARB are larger (= worse precision) because BRYOCARB more fully takes into account the various possible confounding factors. But the BRYOCARB estimates should be more reliable than the empirical ones (= more accurate), especially when applied to fossil settings, because they are underpinned by universal principles, not a series of regional, present-day empirical measurements.

Whether CO₂ was 400 ppm or 500 ppm doesn’t make much of a difference for the authors’ story. The conceptual background of the BRYOCARB model, and the decisions for the inputs used in the model, need to be stated, though.

RE: As above, we seem to be at an impasse due to differing opinions on the utility of BRYOCARB and the empirical model as devised for this study. As such, the CO₂ component of this paper has been removed.

More detailed comments:

Lines 24, 25: Need to say what the uncertainties represent (one-sigma, 95% confidence, etc.).

RE: The CO₂ results have been removed and the information for temperature results has now been added.

Line 25: The reader won’t know what the “theoretical model” is. Some context is needed. Also, is 410 ppm “slightly lower” than 510 ppm (~20% difference)?

RE: The CO₂ component of this paper has been removed.

Lines 28-29: "...promoting taxa increase in abundance." I don't know what this means.

RE: We have added a dash in fire-promoting to clarify that this is an adjective, and also specified examples, *Pinus* and *Picea*.

Line 50: The feedbacks are "engaged", their effects just haven't fully manifested.

RE: The text has been changed as requested.

Line 55: Why is this important?

RE: Now added "for comparability to the modern climate system"

Line 65: What does "it" refer to?

RE: This has been reworded for clarity

Lines 73-74: Would anyone claim that there is a single CO₂ value for the entirety of the Pliocene?? Seems like a straw-man.

RE: They may contend that the addition of a CO₂ estimate from the same site as temperature estimates are taken is not a useful addition because we have many records of CO₂ through the Pliocene, from many proxies already. This points out the issues with using an existing value unless you have very precise age control. This section has been reworked.

Line 145: Remove dash (it looks like a minus sign).

RE: The CO₂ component of this paper has been removed.

Line 146: Why say "However" here? It's not needed.

RE: The CO₂ component of this paper has been removed.

Line 170: Saying "non-vascular mosses" implies that vascular mosses exist.

RE: The CO₂ component of this paper has been removed.

Line 179: The mention of BRYOCARB here comes as a surprise because: 1) it is the first mention of the model and acronym; more context is needed; and 2) the theoretical model has not been properly introduced; equation (1) is not sufficient. Somewhere in the manuscript (or supplement), the choice of inputs needs to be stated and defended. As an aside, Kowalczyk and others recently published an R version of BRYOCARB, which may be more user-friendly (see their supplement):

<https://agupubs.onlinelibrary.wiley.com/doi/abs/10.1029/2018PA003356>

RE: The CO₂ component of this paper has been removed.

Line 196: Was cellulose d13C (not bulk carbon) measured for the extant buckbean? This is not clear. Also, what organs were measured in the extant buckbean? Seeds would make for the best comparison with the fossil seeds.

RE: The CO₂ component of this paper has been removed.

Line 299: Why must these processes be nonlinear?

RE: The CO₂ component of this paper has been removed.

Lines 328, 377, 388: What are these errors? One-sigma?

RE: The CO₂ results have been removed and the information for temperature results has now been added.

Line 331: The uncertainty with the BRYOCARB CO₂ estimate should be asymmetric. Have you computed it correctly?

RE: The CO₂ component of this paper has been removed.

Lines 483-492: This paragraph doesn't seem necessary. There's no need to criticize other methods here.

RE: The CO₂ component of this paper has been removed.

Lines 486-487: The residence time shouldn't matter (other than needing to constrain the boron isotopic composition of sea water). What matters is the relative proportion of the two stable boron isotopes that is incorporated into carbonate minerals.

RE: The CO₂ component of this paper has been removed.

Lines 498: What is the value based on forams?

RE: The CO₂ component of this paper has been removed.

Line 616: "excepted"?

RE: This correction was made.

Line 654: Don't give new information in the Conclusion (Eureka present-day summer temperature).

RE: This information is now introduced earlier in the discussion.

Figure 4: This would be easier to interpret if it were rotated 90 degrees clockwise, so that the vertical axis is age.

RE: This change, along with the deletion of the CO₂ estimates, has been made.

1 Evidence for fire in the Pliocene Arctic in response to amplified temperature

Deleted: f

Deleted: elevated CO₂ and

2 Tamara Fletcher^{1*}, Lisa Warden^{2*}, Jaap S. Sinninghe Damsté^{2,3}, Kendrick J. Brown^{4,5}, Natalia
3 Rybczynski^{6,7}, John Gosse⁸, and Ashley P Ballantyne¹

4 ¹ College of Forestry and Conservation, University of Montana, Missoula, 59812, USA

5 ² Department of Marine Microbiology and Biogeochemistry, NIOZ Royal Netherlands Institute for Sea Research, Den
6 Berg, 1790, Netherlands

7 ³ Department of Earth Sciences, University of Utrecht, Utrecht, 3508, Netherlands

8 ⁴ Natural Resources Canada, Canadian Forest Service, Victoria, V8Z 1M, Canada

9 ⁵ Department of Earth, Environmental and Geographic Science, University of British Columbia Okanagan, Kelowna,
10 V1V 1V7, Canada

11 ⁶ Department of Palaeobiology, Canadian Museum of Nature, Ottawa, K1P 6P4, Canada

12 ⁷ Department of Biology & Department of Earth Sciences, Carleton University, Ottawa, K1S 5B6, Canada

13 ⁸ Department of Earth Sciences, Dalhousie University, Halifax, B3H 4R2, Canada

14 *Authors contributed equally to this work

15 Correspondence to: Tamara Fletcher (tamara.fletcher@umontana.edu)

Deleted: understanding the mechanisms that determine

16 **Abstract.** The mid-Pliocene is a valuable time interval for investigating equilibrium climate at current atmospheric
17 CO₂ concentrations, because atmospheric CO₂ concentrations are thought to have been comparable to current day and
18 yet the climate and distribution of ecosystems was quite different. One intriguing, but not fully understood, feature of
19 the early to mid-Pliocene climate is the amplified arctic temperature response and its impact on arctic ecosystems.
20 Current models underestimate the degree of warming in the Pliocene Arctic and validation of proposed feedbacks is
21 limited by scarce terrestrial records of climate and environment. Here we reconstruct the summer temperature and fire
22 regime from a sub-fossil fen-peat deposit on west-central Ellesmere Island, Canada, that has been chronologically
23 constrained using radionuclide dating to 3.9 +1.5/-0.5 Ma.

Deleted: , as well as discrepancies in current CO₂ proxy reconstructions

Deleted: the CO₂,

24 The estimate for average mean summer temperature is 15.4±0.8°C using specific bacterial membrane lipids, i.e.
25 branched glycerol dialkyl glycerol tetraethers. Macro-charcoal was present in all samples from this Pliocene section
26 with notably higher charcoal concentration in the upper part of the sequence. This change in charcoal was synchronous
27 with a change in vegetation that saw fire-promoting *Pinus* and *Picea* increase in abundance. Paleovegetation
28 reconstructions are consistent with warm summer temperatures, relatively low summer precipitation and an incidence
29 of fire comparable to fire adapted boreal forests of North America, or potentially central Siberia.

Deleted: An empirical transfer function was derived and applied to carbon isotopic measurements of paleo mosses to yield an estimate of Pliocene mean atmospheric CO₂ concentrations of 410 ± 50 ppm, which are slightly lower than theoretical model predictions of 510 ppm.

Deleted:

Deleted: taxa

Formatted: Font: Italic

Formatted: Font: Italic

Deleted: study

Deleted: represents

Deleted: and

Deleted: highlights the important role of forest fire in the ecology and climatic processes of the Pliocene High Arctic

Deleted: The results provide evidence that terrestrial fossil localities in the Pliocene High Arctic were probably formed during warm intervals that coincided with relatively high CO₂ concentrations that supported productive biotic communities.

30 To our knowledge, this site provides the northern-most evidence of fire during the Pliocene. It suggests that ecosystem
31 productivity was much greater, providing fuel for wildfires, and that the climate was conducive to the ignition of fire
32 during this period. This study indicates that interactions between paleovegetation and paleoclimate were mediated by
33 fire in the High Arctic during the Pliocene, even though CO₂ concentrations were similar to modern.

Deleted: almost double

34 1 Introduction

35 Current rates of warming in the Canadian Arctic are now roughly triple the rate of global warming (Bush and Lemmen,
36 2019). Since 1850, global land surface temperatures have increased by approximately 1.0°C, whereas circum-arctic

60 land surface temperatures have increased by $\geq 2.0^{\circ}\text{C}$ (Jones and Moberg, 2003; Francis and Skific, 2015). Such arctic
61 amplification of temperatures has also occurred during other warm climate anomalies in Earth's past. Paleoclimate
62 records from the Arctic indicate that the change in arctic summer temperatures during past global warm periods was
63 3–4 times larger than global temperature change (Miller et al., 2010). While the latest ensemble of earth system models
64 (ESMs) provide fairly accurate predictions of the modern amplification of arctic temperatures hitherto observed
65 (Marshall et al., 2014), they often under-predict the amplification of arctic temperatures during past warm intervals in
66 Earth's history, including the Eocene (33.9–56 Ma; Shellito et al., 2009), and the Pliocene (2.6–5.3 Ma; Dowsett et
67 al., 2012; Salzmann et al., 2013) epochs. These differences suggest that either the models are not simulating the full
68 array of feedback mechanisms properly for past climates, or that the full array of fast and slow feedback mechanisms
69 have not manifested for the modern Arctic. If the later, the Arctic region and its ecosystems have yet to reach a new
70 equilibrium in response to full temperature amplification.

71 The Pliocene is an intriguing climatic interval that may offer important insights into climate feedbacks. Atmospheric
72 CO_2 concentrations were, at times, as high as modern (Fig. 1), but generally show a decreasing trend throughout the
73 Pliocene (Haywood et al., 2016; Pagani et al., 2010; Royer et al., 2007; Stap et al., 2016). Although CO_2 estimates
74 from different methods do not converge, the modelled direct effects of these CO_2 discrepancies appear to be small
75 (Feng et al., 2017). Of additional importance for comparability to the modern climate system, continental
76 configurations were similar to present (Dowsett et al., 2016). While global mean annual temperatures (MATs) during
77 the Pliocene were only $\sim 3^{\circ}\text{C}$ warmer than present day, arctic land surface MATs may have been as much as 15 to
78 22°C warmer (Ballantyne et al., 2010; Csank et al., 2011a; Csank et al., 2011b; Fletcher et al., 2017). Further, arctic
79 sea surface temperatures may have been as much as 10 to 15°C warmer than modern (Robinson, 2009), and sea-levels
80 were approximately 25m higher than present (Dowsett et al., 2016). As a result, the Arctic terrestrial environment was
81 significantly different from today, with boreal ecosystems at much higher latitudes (Salzmann et al., 2008). These
82 changes in vegetation due to climate, may have also provided further important feedbacks to arctic temperatures (e.g.
83 Otto-Bliesner and Upchurch Jr, 1997).

84 To advance our understanding of arctic ecosystem response and feedback to temperature amplification during past
85 warm intervals in Earth's history this investigation targets an exceptionally well-preserved arctic sedimentary
86 sequence to simultaneously reconstruct summer temperature, vegetation and fire from a single site.

87 2 Methods

88 2.1 Site description

89 To investigate the environment and climate of the Pliocene Arctic we focused on the Beaver Pond (BP) fossil site,
90 located at $78^{\circ} 33' \text{N}$ (Fig. 2) on Ellesmere Island. The stratigraphic section located at ~ 380 meters above sea level
91 (MASL) today includes unconsolidated bedded sands and gravels, and rich organic layers including a fossil rich peat
92 layer, up to 2.4 m thick, with sticks gnawed by an extinct beaver (*Dipoides spp.*). The assemblage of fossil plants and
93 animals at BP has been studied extensively to gain insight into the past climate and ecology of the Canadian High
94 Arctic (Ballantyne et al., 2006; Csank et al., 2011a; Csank et al., 2011b; Fletcher et al., 2017; Mitchell et al., 2016;

Deleted: Pagani et al., 2010,

Deleted: Huber, 2008;

Deleted: fully engaged

Deleted: s

Deleted: the full

Deleted: potential demonstrated in the past

Deleted: values varied

Deleted: Royer et al., 2007) decreasing from values comparable to modern (

Deleted:), to lower levels (Raymo et al., 2006

Deleted:); a state transition that may revert in the future under high CO_2

Deleted: (Fig. 1),

Deleted: 0

Deleted: such,

Deleted: of the Arctic

Deleted: tree line

Deleted: nearly eliminating the tundra biome

Deleted: ¶

Deleted: Several mechanisms have been proposed as drivers of arctic amplification, including vastly reduced sea-ice extent (Ballantyne et al., 2013), cloud and atmospheric water vapor effects (e.g. Feng et al., 2016; Swann et al., 2010), vegetation controls on albedo (Otto-Bliesner and Upchurch Jr, 1997), and increased meridional heat transport by the oceans (Dowsett et al., 1992) though it is now considered to be of lesser influence (Hwang et al., 2011). We propose that fire in arctic ecosystems may also be an important mechanism for amplifying arctic surface temperatures during the Pliocene, and so seek to understand its characteristics through quantification from the sediment record. ¶

—Although it is generally thought that atmospheric CO_2 concentrations of ~ 400 ppm provided the dominant global radiative forcing during the mid-Pliocene, CO_2 proxies over the Pliocene do not all agree (Fig. 1). Reconstructions of Pliocene CO_2 range between 190 and 440 ppm (Martinez-Boti et al., 2015; Seki et al., 2010). While CO_2 estimates from stomata and paleosols tend to be less precise, they are within the range of boron and alkenone derived estimates (Royer, 2006; Foster et al. 2017). Due to this variation in estimates from approximately the same time and variation in CO_2 over time, there is no clear value for CO_2 concentration in Earth's atmosphere that can be assigned to broad periods during the Pliocene. Dating uncertainties are an additional confounding factor complicating site to site comparison. Although modelled direct effects of this level of CO_2 variation may be small (Feng et al., 2017), reconstructing the CO_2 from the same deposits from which paleoclimate and paleoecological proxies are derived, may help reconcile previous estimates and contribute to constraining climate sensitivities during the Pliocene.

Formatted: Subscript

Deleted: such as the Pliocene by providing data to support boundary conditions and for verification in ESMs,

Deleted: atmospheric CO_2 ,

Deleted: p

147 Rybczynski et al., 2013; Tedford and Harington, 2003; Wang et al., 2017). Previous paleoenvironmental evidence
148 suggests the main peat unit is a rich fen deposit with a neutral to alkaline pH, associated with open water (Mitchell et
149 al., 2016), likely a lake edge fen or shallow lake fen, within a larch-dominated forest-tundra environment (Matthews
150 and Fyles, 2000), not a low pH peat-bog. While the larch species identified at the site, *Larix groenlandia*, is extinct
151 (Matthews and Fyles, 2000), many other plant remains are Pliocene examples of taxa that are extant (Fletcher et al.,
152 2017).

153 The fen-peat unit examined in this study was sampled in 2006 and 2010. The main sequence examined across the
154 methods used in this study includes material from Unit II, the entire span of Unit III, and material from Unit IV
155 sampled from Section A as per Mitchell et al. (2016; Fig. S1; see Mitchell et al. 2016 Fig 5), with a total sampled
156 profile of 1.65 m. Unit III has been estimated to represent ~20 000 years of deposition based on modern northern fen
157 accumulation rates (Mitchell et al., 2016). The charcoal estimates from this locality were based on 31 sample layers
158 from the 2006 field campaign, while the temperature estimates from specific bacterial membrane lipids were taken
159 from 22 of the sample layers collected in 2006 and an additional 12 samples collected in 2010. The same samples
160 from the 2006 season were analyzed for mean summer temperature and char count where contents of the sample
161 allowed. Pollen was tabulated from 10 samples from the 2006 sequence, located at different stratigraphic depths.

Deleted: growth

Deleted: atmospheric

Deleted: CO₂

Deleted: 22

Deleted: , and the charcoal was based on 31

Deleted: each of CO₂,

162 2.2 Geochronology

163 While direct dating of the peat was not possible, we were able to establish a burial age for fluvial sediments deposited
164 approximately 4–5 m above and 30 m to the southwest of the peat. We used a method based on the ratio of isotopes
165 produced in quartz by secondary cosmic rays. The cosmogenic nuclide burial dating approach measures the ratio of
166 cosmogenic ²⁶Al (t_{1/2} = 0.71 Ma) and ¹⁰Be (t_{1/2} = 1.38 Ma) in quartz sand grains that were exposed on hillslopes and
167 alluvium prior to final deposition at BP. Once the quartz grains are completely shielded from cosmic rays, the ratio of
168 the pair will predictably decrease because ²⁶Al has double the radiodecay rate of ¹⁰Be. In 2008, four of the medium to
169 coarse grained quartz samples were collected from a vertical profile of planar crossbedded fluvial sands between 8.7
170 and 10.4 m below the overlying till surface. The samples were 5 cm thick, separated by an average of 62 cm, and
171 should closely date the peat (the sandy braided stream beds represent on the order of ~10⁴ years from the top of the
172 peat to the highest sample). Quartz concentrates were extracted from the arkosic sediment using Frantz magnetic
173 separation, heavy liquids, and differential leaching with HF in ultrasonic baths. When sample aliquots reached
174 aluminum concentrations <100 ppm (ICP-OES) as a proxy of feldspar abundance, the quartz concentrate was
175 subjected to a series of HF digestion and rinsing steps to ensure that more than 30% of the quartz had been dissolved
176 to remove meteoric ¹⁰Be. Approximately 200 mg of Be extracted from a Homestake Gold Mine beryl-based carrier
177 was added to 150 g of each quartz concentrate (no Al carrier was needed for these samples). Such large quartz masses
178 were digested because of the uncertainty in the abundance of the faster decaying isotope. Following repeated
179 perchloric-acid dry-downs to remove unreacted HF, pH-controlled precipitation, column chemistry ion
180 chromatography to extract the Be and Al ions, precipitation in ultrapure ammonia gas, and calcination at temperatures
181 above 1000°C in a Bunsen flame for three minutes, oxides were mixed with equal amounts of niobium and silver by
182 volume. These were packed into stainless steel targets for measurement at Lawrence Livermore National Laboratory's

189 accelerator mass spectrometer (AMS). Uncertainty estimates for $^{26}\text{Al}/^{10}\text{Be}$ were calculated as 1σ by combining AMS
 190 precision with geochemistry errors in quadrature. For a complete detailed description of TCN methods see Rybczynski
 191 et al. (2013). The ages provided here are updated from Rybczynski et al. (2013) by using more recent production rate
 192 information and considering the potential for increasing exposure to deeply penetrating muons during the natural post-
 193 burial exhumation at BP.

194 2.3 Paleotemperature Reconstruction

195 Paleotemperature estimates were determined based on the distribution of fossilized, sedimentary membrane lipids
 196 known as branched glycerol dialkyl glycerol tetraethers (brGDGTs) that are well preserved in peat bogs, soils, and
 197 lakes (Powers et al., 2004; Weijers et al., 2007c). These unique lipids are thought to be synthesized by a wide array of
 198 Acidobacteria within the soil (Sinninghe Damsté et al., 2011; Sinninghe Damsté et al., 2014) and presumably other
 199 bacteria (Sinninghe Damsté et al., 2018) in soils and peat bogs but also in aquatic systems. Previously, it has been
 200 established that the degree of methyl branching (expressed in the methylation index of branched tetraethers; MBT) is
 201 correlated with mean annual air temperature (MAAT), and the relative amount of cyclopentane moieties (expressed
 202 in the cyclization index of branched tetraethers; CBT) has been shown to correlate with both soil pH and MAAT
 203 (Weijers et al., 2007b). Because of the relationship of the distribution of these fossilized membrane lipids with these
 204 environmental parameters, it has been used for paleoclimate applications in different environments including coastal
 205 marine sediments (Bendle et al., 2010; Weijers et al., 2007a), peats (Ballantyne et al., 2010; Naafs et al., 2017),
 206 paleosols (Peterse et al., 2011; Zech et al., 2012), and lacustrine sediments (Loomis et al., 2012; Niemann et al., 2012;
 207 Pearson et al., 2011; Zink et al., 2010). [In this study we reconstruct mean summer air temperature \(MST\), using a](#)
 208 [modified version of a calibration that was developed by Pearson et al. \(2011\) and is based on 90 core top lacustrine](#)
 209 [sediment samples from diverse climates and geographical areas.](#)

210 Improved separation methods (Hopmans et al., 2016) have recently led to the separation and quantification of the 5-
 211 and 6-methyl brGDGT isomers that used to be treated as one since the 6-methyl isomers were co-eluting with the 5-
 212 methyl isomers (De Jonge et al., 2013). This has led to the definition of new indices and improved MAAT calibrations
 213 based on the global soil (De Jonge et al., 2014), peat (Naafs et al., 2017), and African lake (Russell et al., 2018)
 214 datasets.

215 Sediment samples were freeze-dried and then ground and homogenized with a mortar and pestle. Next, using the
 216 Dionex™ accelerated solvent extractor (ASE), 0.5–1.0 g of sediment was extracted with the solvent mixture of
 217 dichloromethane (DCM):methanol (9:1, v/v) at a temperature of 100°C and a pressure of 1500 psi (5 min each) with
 218 60% flush and purge 60 s. The Caliper Turbovap®LV was utilized to concentrate the collected extract, which was
 219 then transferred using DCM and dried over anhydrous Na_2SO_4 before being concentrated again under a gentle stream
 220 of N_2 gas. To quantify the amount of GDGTs, 1 μg of an internal standard (C46 GDGT; Huguet et al., 2006) was
 221 added to the total lipid extract. Then, the total lipid extract was separated into three fractions using hexane:DCM (9:1,
 222 v:v) for the apolar fraction, hexane:DCM (1:1, v:v) for the ketone fraction and DCM:MeOH (1:1, v:v) for the polar
 223 fraction, using a column composed of Al_2O_3 , which was activated for 2 h at 150°C. The polar fraction, which contained
 224 the GDGTs, was dried under a steady stream of N_2 gas and weighed before being re-dissolved in hexane:isopropanol

Deleted: Atmospheric CO₂ Reconstruction

In order to reconstruct atmospheric CO₂ concentrations during the Pliocene, we derived a method based on the different sensitivity of isotopic discrimination of plant groups to their environment (Farquhar et al., 1989; Fletcher et al., 2008; White et al., 1994). Specifically, we used measurements of stable carbon isotopic discrimination in C3 vegetation to approximate the carbon isotopic signature of the atmosphere, and measurements of carbon isotopic discrimination in bryophytes to estimate the partial pressure of atmospheric CO₂, which was then converted to atmospheric CO₂ concentration. According to theory (Farquhar et al., 1989), plants discriminate ($\Delta^{13}\text{C}$) against the heavier isotope in atmospheric CO₂, such that:

$$\Delta^{13}\text{C} = a + (b - a) \frac{p_i}{p_a} \quad (1)$$

where the fractionations of atmospheric CO₂ due to diffusion ($a = \sim -4.4\text{‰}$) and carboxylation by the enzyme rubisco ($b = \sim -27\text{‰}$) are constraints. Thus, isotopic fractionation in C3 plants ($\Delta^{13}\text{C}_{\text{C3}}$) is largely a function of stomatal control of partial pressure of intercellular CO₂ (p_i) with respect to the partial pressure of atmospheric CO₂ (p_a). However, bryophytes lack stomata and thus a mechanism for actively regulating p_i , such that isotopic fractionation ($\Delta^{13}\text{C}_{\text{bry}}$) varies mainly as a function of partial pressure in atmospheric CO₂ (i.e. p_a). While other environmental factors, such as humidity, temperature, light availability, and microclimate may also play important roles in isotopic discrimination in bryophytes (Fletcher et al., 2008; Ménot and Burns, 2001; Royles et al., 2014; Skrzypek et al., 2007; Waite and Sack, 2011; White et al., 1994), the first order control on discrimination is the partial pressure of atmospheric CO₂ (Fletcher et al., 2008; White et al., 1994). Because atmospheric CO₂ is relatively well mixed in the troposphere its mean annual concentration does not differ significantly by location. However, because total atmospheric pressure decreases with atmospheric height (h), the partial pressure of atmospheric CO₂ must also decrease according to the following exponential function:

$$p_a(h) = p_a(i) e^{-h/H} \quad (2)$$

such that the partial pressure of atmospheric CO₂ at any given height in the atmosphere ($p_a(h)$) can be calculated based on the initial atmospheric partial pressure of atmospheric CO₂ ($p_a(i)$) and a reference height ($H = 7600$ m), where atmospheric pressure goes to 0.37 Pa (Bonan, 2015). Therefore, assuming that carbon isotopic discrimination in bryophytes varies in response to the partial pressure of atmospheric CO₂ we can predict from basic physical principles an increase in $\Delta^{13}\text{C}_{\text{bry}}$ in response to an increase in $p_a(h)$. Furthermore, if the assumptions of this empirical relationship are valid, then this empirical relationship can in theory be used to predict the partial pressure of atmospheric CO₂ based on carbon isotopic measurements of bryophytes.

To test this prediction, we compiled data from four studies investigating carbon isotopic variability of different bryophytes, primarily mosses, along elevational transects at different locations. Based on the elevations and locations of moss samples, the atmospheric partial pressure of atmospheric CO₂ was estimated from ERA-interim reanalysis data of total atmospheric pressure (Dee et al., 2011) in conjunction with globally averaged atmospheric CO₂ concentrations (Global View-CO₂, 2013) from the years moss samples were collected. For our analysis we only included measurements of carbon isotopic variability in non-vascular mosses and all isotopic values were normalized to ... [1]

Deleted: mean annual air temperature

Deleted: i

Deleted: n

Deleted: then

374 (99:1, v:v) at a concentration of 10 mg ml⁻¹ and subsequently passed through a 0.45 µm PTFE filter. Finally, the polar
 375 fractions were analyzed for GDGTs by ultra-high performance liquid chromatography – atmospheric pressure positive
 376 ion chemical ionization – mass spectrometry (UHPLC-APCI-MS) using the method described by Hopmans et al.,
 377 (2016). The polar fractions of some samples were re-run on the UHPLC-APCI-MS multiple times and the average
 378 fractional abundances of the brGDGTs was determined.

379 For the calculation of brGDGT-based proxies, the brGDGTs are specified by the Roman numerals as indicated in
 380 Fig. S2. The 6-methyl brGDGTs are distinguished from the 5-methyl brGDGTs by a prime. The novel indices,
 381 including MBT'_{5Me} based on just the 5-methyl brGDGTs and the CBT' that was used to calculate the pH (De Jonge et
 382 al., 2014):

383
 384 $MBT'_{5Me} = ([Ia] + [Ib] + [Ic]) / ([Ia] + [Ib] + [Ic] + [IIa] + [IIb] + [IIc] + [IIIa] + [IIIb] + [IIIc])$ (1)

385 $CBT' = -^{10}\log\left(\frac{[Ic] + [IIa'] + [IIb'] + [IIc'] + [IIIa'] + [IIIb'] + [IIIc']}{[Ia] + [IIa] + [IIIa]}\right)$ (2)

386
 387 The square brackets denote the fractional abundance of the brGDGT within the bracket relative to the total brGDGTs.

388 The distributions of aquatically produced brGDGTs in the lake calibration developed by Pearson et al. (2011) were
 389 used to determine MST. When this calibration is used the fractional abundances of IIa and IIa' must be summed
 390 because these two isomers co-eluted under the chromatographic conditions used by Pearson et al. (2011):

391
 392 $MST (^{\circ}C) = 20.9 + 98.1 \times [Ib] - 12 \times ([IIa] + [IIa']) - 20.5 \times [IIIa]$, RMSE = 2.0°C (3)

393
 394 MAAT and surface water pH were also calculated using a novel calibration created using sediments from East African
 395 lakes analysed with the novel chromatography method and based upon MBT'_{5Me} (Russell et al., 2018).

396
 397 $MAAT = -1.2141 + 32.4223 * MBT'_{5Me}$ RMSE of 2.44 °C (4)

398 $Surface\ water\ pH = 8.95 + 2.65 * CBT'$ RMSE of 0.80 (5)

399 **2.4 Vegetation and Fire Reconstruction**

400 For charcoal, a total of thirty 2 cm³ samples were taken at 5 cm intervals from depths from 380 and 381.45 MASL at
 401 the BP site, with an additional 2cm⁻³ sample collected at 381.65 MASL. All samples were deflocculated using sodium
 402 hexametaphosphate and passed through 500, 250 and 125 µm nested mesh sieves. The residual sample caught on each
 403 sieve was then collected in a gridded petri dish and examined using a stereomicroscope at 20-40X magnification to
 404 obtain charcoal concentration (fragments cm⁻³). Charcoal area (mm² cm⁻³) was measured for each sample using
 405 specialized imaging software from Scion Corporation. For a detailed description of methods see Brown and Power
 406 (2013).

407 Vegetation was reconstructed using pollen and spores (herein pollen) at selected elevations chosen to capture upper
 408 and lower sections of the elevation profile, and that corresponded with changes in charcoal. The sample depths selected
 409 for pollen analyses were 380.3–380.4 MASL, 381.10–381.25 MASL, and 381.35–381.45 MASL. Samples were

Deleted: 4

Deleted: 5

Deleted: Mean summer air temperature (MST) was determined using

Deleted: t

Deleted: →

Deleted: →

Deleted: 6

Deleted: →

Deleted: →

Deleted: 7

Deleted: →

Deleted: 8

Deleted: 5

Deleted: 0

Deleted: 0

Deleted: 0

Deleted: 0

Deleted: 0

Deleted: 0

Deleted: 0

Deleted: 0

Deleted: 0

433 processed using standard approaches (Moore et al., 1991), whereby 1cm³ sediment subsamples were treated with 5%
 434 KOH to remove humic acids and break up the samples. Carbonates were dissolved using 10% HCl, whereas silicates
 435 and organics were removed by HF and acetolysis treatment, respectively. Pollen slides were made by homogenizing
 436 35 µl of residue, measured using a single-channel pipette, with 15 µl of melted glycerin jelly. Slides were counted
 437 using a Leica DM4000 B LED compound microscope at 400–630x magnification. A reference collection and
 438 published keys (McAndrews et al., 1973; Moore et al., 1991) aided identification.

439 In addition to tabulating pollen and charcoal, a list of plant taxa derived from Beaver Pond was previously compiled
 440 in Fletcher et al. (2017). Extant species from this list were selected and their modern occurrences extracted from the
 441 Global Biodiversity Information Facility (GBIF.org, 2017). Observation data was grouped by 5° latitude 5° longitude
 442 grids cells, and the shared species count calculated using R (R Core Team, 2016). Modern fire frequency was mapped
 443 using the MODIS 6 Active Fire Product. The fire pixel detection count per day, within the same 5° latitude 5° longitude
 444 grids cells was counted over the ten years 2006–2015, and standardized by area of the cell. The modern climate maps
 445 were generated using data from WorldClim 1.4 (Hijmans et al., 2005). The values for the bioclimatic variables mean
 446 temperature of the warmest quarter (equivalent to \overline{MST}) and precipitation of the warmest quarter (summer
 447 precipitation) were also averaged by grid cell. The shared species count, climate values, and fire day detections were
 448 mapped to the northern polar stereographic projection in ArcMap 10.1.

449 3 Results

450 3.1 Geochronology

451 The burial dating results with ²⁶Al/¹⁰Be in quartz sand at 10 m below modern depth provides four individual ages.
 452 From shallowest to deepest, the burial ages are 3.6 +1.5/-0.5 Ma, 3.9 +3.7/-0.5 Ma, 4.1 +5.8/-0.4 Ma, and 4.0 +1.5/-
 453 0.4 Ma (Table S2), with an unweighted mean age of 3.9 Ma. The convoluted probability distribution function yields
 454 a maximum probability age of 4.5 Ma. Unfortunately, the positive tails of the probability distribution functions of two
 455 of the samples exceeds the radiodecay saturation limit of the burial age. Therefore, their probability distributions do
 456 not reflect the actual age probabilities and uncertainty. Given the positive tail in the probability distribution functions,
 457 and the inability to convolve all samples, we recommend using the unweighted mean age, 3.9 Ma, with an uncertainty
 458 of +1.5/-0.5 Ma as indicated by the two samples with unsaturated limits. Despite the apparent upward younging of the
 459 individual burial ages, the 1σ-uncertainties overlap rendering the samples indistinguishable.

460 3.2 Paleotemperature Estimates

461 3.2.1 Provenance of branched GDGTs

462 Previously, brGDGT derived MAAT estimates (-0.6 ± 5.0 °C) from BP sediments were developed using the older
 463 chromatography methods that did not separate the 5- and 6- methyl brGDGTs, and a soil calibration (Ballantyne et
 464 al., 2010). In marine and lacustrine sediments, bacterial brGDGTs were thought to originate predominantly from
 465 continental soil erosion arriving in the sediments through terrestrial runoff. More recent studies, however, have
 466 indicated aquatically produced brGDGTs could be affecting the distribution of the sedimentary brGDGTs and thus

Deleted: mean summer air temperature;

Deleted: Atmospheric CO₂ Reconstruction

As expected, carbon isotopic discrimination in mosses shows a positive relationship with partial pressure of atmospheric CO₂ both in empirical observations and theoretical predictions (Fig. 3). However, a much greater change in Δ¹³C_{mos} is observed in response to p_a than is predicted from the optimized BRYOCARB simulations. The empirical fit to the observed change in Δ¹³C_{mos} in response to p_a is slightly better (RMSE = 1.8 ‰) than the theoretical prediction from the BRYOCARB model (RMSE = 2.1 ‰), but the slopes are quite different, with our empirical slope (0.56 ‰/ p_a) an order of magnitude greater than the linear approximation of the BRYOCARB slope (0.07 ‰/ p_a), suggesting that other non-linear processes and not just p_a may be affecting δ¹³C_{mos} variability with elevation.

While there does appear to be a global relationship between p_a and Δ¹³C of mosses, there are notable differences among sites. Moss Δ¹³C values tended to be generally lower in the Swiss Alps (mean = 17.4 ‰) and higher in Hawaii (mean = 20.6 ‰) and the slope of the relationship between p_a and Δ¹³C appears to vary across sites with the Andes having the smallest slope and Poland having a much greater slope. We used the BRYOCARB model to test the sensitivity of Δ¹³C to other variables that change as a function of elevation (e.g. temperature and pO_2). According to our BRYOCARB simulations, with all other variables held constant decreased temperature with increased elevation should slow metabolic rates resulting in an increase in Δ¹³C (Fig. S3), which directly contradicts observations (Fig. 3). Furthermore, the range of mean summer temperature estimates from the Pliocene BP site could only explain ~0.2 ‰ isotopic response in our moss samples. Similarly we evaluated the effect of just changing pO_2 in our BRYOCARB simulations and found a decrease in Δ¹³C with increasing pO_2 that is opposite to the Δ¹³C response of mosses to partial pressure across all elevational transects. We also evaluated model performance using a global standard atmospheric sea level pressure of 101.325 kPa, or site-specific atmospheric pressure estimates from ERA-interim reanalysis data. We found that the model using site specific atmospheric pressure estimates performed better at predicting Δ¹³C_{mos} (RMSE = 1.096 ‰) than the model using global standard atmospheric sea level pressure (RMSE = 1.216 ‰). Therefore, it appears that partial pressure of atmospheric CO₂ is the primary physical mechanism explaining the global relationship between Δ¹³C of mosses and elevation and that other factors, such as water availability that may be mediated by different lapse rates (Ménot and Burns, 2001; Royles et al., 2014; Skrzypek et al., 2007; Waite and Sack, 2011), may explain variability among sites. Thus, the optimal model characterizing the observed modern relationship between Δ¹³C_{mos} and the p_a was:

$$^{13}C \Delta^{13}C_{mos} = 0.56 \times pCO_2 + 1.55 \text{ (9)}$$

Based on our analysis of cellulose extracted from four different *Menyanthes L.* (i.e. buckbean) plants growing at four different locations in the modern boreal forest, we found Δ¹³C of buckbean to be fairly constant 16 ± 0.4 ‰, yielding an estimate of p_i/p_a in modern buckbean of 0.51. Applying this modern of p_i/p_a to our δ¹³C measurements from sub-fossil buckbean we obtained estimates of δ¹³C_{atm} during the Pliocene of -6.23 ± 0.9 ‰. Using our empirical transfer function (Eq. 9) in combination with these estimates of δ¹³C_{atm}, we were able to approximate atmospheric CO₂ concentrations over the Pliocene interval captured at the BP site (Fig. 4). We estimated a mean atmospheric CO₂ ... [2]

Deleted: 3

Deleted: ,

Deleted: however, a number of

Deleted: m

608 the temperature estimates based upon them (Warden et al., 2016; Zell et al., 2013; Zhu et al., 2011). Since the discovery
609 that sedimentary brGDGTs can have varying sources, different calibrations have been developed depending on the
610 origin of the brGDGTs, i.e. soil calibration (De Jonge et al., 2014), peat calibration (Naafs et al., 2017) and aquatic
611 calibrations (i.e. Foster et al., 2016; Pearson et al., 2011; Russell et al., 2018). Therefore, several studies have
612 recommended that the potential sources of the sedimentary brGDGTs should be investigated before attempting to use
613 brGDGTs for paleoclimate applications (De Jonge et al., 2015; Warden et al., 2016; Yang et al., 2013; Zell et al.,
614 2013). In this study, we examine the distribution of brGDGTs in an attempt to determine their origin and consequently
615 the most appropriate calibration to utilize in order to reconstruct temperatures from the BP sediments.

616 Branched GDGTs IIIa and IIIa' on average had the highest fractional abundance of the brGDGTs detected in the BP
617 sediments (see Fig. S2 for structures; Table S4). A previous study established that when plotted in a ternary diagram
618 the fractional abundances of the tetra-, penta- and hexamethylated brGDGTs, soils lie within a distinct area (Sinninghe
619 Damsté, 2016). To assess whether the brGDGTs in the BP deposit were predominantly derived from soils, we
620 compared the fractional abundances of the tetra-, penta- and hexamethylated brGDGTs in the BP sediments to those
621 from modern datasets in a ternary diagram (Fig. 3). Since the contribution of brGDGTs from either peat or aquatic
622 production could affect the use of brGDGTs for paleoclimate application, in addition to comparing the samples to the
623 global soil dataset (De Jonge et al., 2014), peat and lacustrine sediment samples were added into the ternary plot to
624 help elucidate the provenance of brGDGTs in the BP sediments. According to Sinninghe Damsté (2016), it is
625 imperative to only compare samples in a ternary diagram like this where all of the datasets were analyzed with the
626 novel methods that separate the 5- and 6-methyl brGDGTs since the improved separation can result in an increased
627 quantification of hexamethylated brGDGTs. Recently, samples from East African lake sediments were analyzed using
628 these new methods (Russell et al., 2018) and so these samples were included in the ternary plot for comparison (Fig.
629 3). Although the lakes from the East African dataset are all from a tropical area, they vary widely in altitude and, thus,
630 in MAAT. We separated them into three categories by MAAT (lakes >20°C, lakes between 10-20°C and lakes <10°C).
631 By comparing all the samples in the ternary plot, it was evident that the BP samples plotted closest to the lacustrine
632 sediment samples from regions in East Africa with a MAAT <10°C, suggesting that the provenance of the majority
633 of the brGDGTs from the BP sediments was not soil or peat but lacustrine aquatic production.

634 The average estimated surface water pH for the BP sediments (8.6 ± 0.2) calculated using eq. (5), is within the 6–9
635 range typical of lakes and rivers (Mattson, 1999). This value is near the upper limit of rich fens characterized by the
636 presence of *S. scorpioides* (Kooijman and Westhoff, 1995; Kooijman and Paulissen, 2006) and is higher than what
637 would be expected for peat-bog sediments that are acidic (pH 3–6; Clymo, 1964) and which constitute most of the
638 peats studied by Naafs et al. (2017). A predominant origin from lake aquatic production is in keeping with previous
639 interpretation of the paleoenvironment of the BP site, which was at least at times covered by water as evidenced by
640 fresh water diatoms, fish remains and gnawed beaver sticks in the sediment (Mitchell et al., 2016).

641 3.2.2 Aquatic Temperature Transfer Function

642 Since there is evidence that the majority of the brGDGTs in the BP sediments are aquatically produced, an aquatic
643 transfer function was used for reconstructing temperature. When we apply the African lake calibration (Eq. 4), the

Deleted: 5

Deleted: abundance

Deleted: 5

Deleted: 8

Deleted: 3

Deleted: 7

650 resulting estimated MAAT for BP is 7.1 ± 1.0 °C (mean \pm standard deviation). This value is high compared to other
 651 previously published estimates from varying proxies, which have estimated MAAT in this region to be in the range
 652 of -5.5 to 0.8°C, (Ballantyne et al., 2010; Ballantyne et al., 2006; Csank et al., 2011a; Csank et al., 2011b; Fletcher et
 653 al., 2017). A concern when applying this calibration is that it is based on lakes from an equatorial region that does not
 654 experience substantial seasonality, whereas, the Pliocene Arctic BP site did experience substantial seasonality
 655 (Fletcher et al., 2017). Biological production (including brGDGT production) in BP was likely skewed towards
 656 summer and, therefore, summer temperature has a larger influence on the reconstructed MAAT. Unfortunately, no
 657 global lake calibration set using individually quantified 5- and 6-methyl brGDGTs is yet available. Therefore, to
 658 calculate MST (Eq. 3) we applied the aquatic transfer function developed by Pearson et al. (2011) by combining the
 659 individual fractional abundances of the 5- and 6-methyl brGDGTs. The Pearson et al. (2011) calibration was based on
 660 a global suite of lake sediments including samples from the Arctic, thus covering a greater range of seasonal
 661 variability. The resulting average estimated MST was 15.4 ± 0.8 °C (average \pm standard deviation), with temperatures
 662 ranging between 14.1 and 17.4 °C (Fig. 4). This is in good agreement with recent estimates based on Climate
 663 Reconstruction Analysis using Coexistence Likelihood Estimation (CRACLE; Fletcher et al., 2017) that concluded
 664 that MSTs at BP during the Pliocene were approximately 13 to 15°C.

665 3.3 Vegetation and Fire Reconstruction

666 All sediment samples from BP contained charcoal (Fig. 4), indicating the consistent prevalence of biomass burning in
 667 the High Arctic during this time period. However, counts were variable throughout the section, with the middle and
 668 lower sections (mean 34 fragments cm⁻³) containing less charcoal compared to the upper section upper section (mean
 669 444 fragments cm⁻³). Overall, samples from BP contained on average 100.0 ± 165 fragments cm⁻³ (mean \pm 1 σ), with
 670 charcoal area averaging 12.3 ± 20.2 mm² cm⁻³. The variability of charcoal within any given sample was relatively low
 671 with a 1 σ among charcoal area of approximately 2 mm² cm⁻³.

672 The three parts of the section analysed for pollen (380.3–380.4 MASL, 381.15–381.25 MASL, and 381.35–381.45
 673 MASL) reveal variations in vegetation (Figs. 4 and 5). Near the bottom of the section (380.3–380.4 MASL), *Larix*
 674 (26%) and *Betula* (17%) were the dominant trees. *Alnus* (6%) and *Salix* (6%) together with ericaceous pollen (4%)
 675 were relatively high. In contrast, low numbers of *Picea* (3%), *Pinus* (3%) and fern spores were recorded. Additional
 676 wetland taxa like *Myrica* (5%) and Cyperaceae (6%) were also noted. Overall, the non-arboreal (23%) signal was well
 677 developed. Crumpled and/or ruptured inaperturate grains with surface sculpturing that varied from scabrate to
 678 verrucate were noted in the assemblage (12%), but could not be definitely identified. It is possible that these grains
 679 represent *Populus*, Cupressaceae or additional Cyperaceae pollen. Between 381.10–381.25 MASL, *Larix* (38%) and
 680 *Betula* (21%) increased in abundance, followed by ferns (7%). Cyperaceae remained at similar levels (6%) whereas
 681 *Picea* and *Pinus* decreased to 2% and 1%, respectively. Unidentified inaperturate types collectively averaged 14%.
 682 *Larix* pollen (23%) remained abundant near the top of the section (381.35–381.45 MASL), whereas *Betula* (2%)
 683 decreased. *Picea* (16%) *Pinus* (6%) and ferns (23%) increased in abundance. Of the ferns, trilete spores and cf.
 684 *Botrychium* were most abundant, followed by cf. *Dryopteris*. Inaperturate unknowns (10%) were also observed. Other
 685 notables included Ericaceae (2%) and Cyperaceae (2%). While rare, Onagraceae grains were also observed (Fig. 5).

Deleted: mean summer air temperatures (

Deleted: ,

Deleted: 6

Deleted: mean summer temperature

Deleted: 4

Deleted: 4

Deleted: 18

Deleted: 710

Deleted: 0

Deleted: 0

Deleted: 0

Deleted: 0

Deleted: 0

Deleted: 0

Deleted: 6

Deleted: 0

Deleted: 0

Deleted: 0

Deleted: 0

Deleted: 0

Deleted: 0

Deleted: 6

708 According to [the](#) GBIF-based mapping exercise, the paleofloral assemblage at BP most closely resembles modern
709 vegetation found in northern North America, particularly on the eastern margin (e.g. New Hampshire, New Brunswick
710 and Nova Scotia) and the western margin (Alaska, Washington, British Columbia, and Alberta; Fig. 7a), and central
711 Fennoscandia. Of these areas, the western coast of northern North America and eastern coast of southern Sweden has
712 the most similarity to the reconstructed BP climate in terms of MST (Fig. 7b) and summer precipitation (Fig. 7c).

713 While high counts of active fire days are common in the western part of the North American boreal forest, it is not
714 as common in the eastern part of the North American boreal forest (Fig. 7d), likely due to the differences in the
715 precipitation regime. There were also low fire counts in Fennoscandia likely due to historical severe fire suppression
716 (Brown and Giesecke, 2014; Niklasson and Granström, 2004). Therefore, based on our reconstruction of the climate
717 and ecology of the BP site, our results suggest that BP most closely resembled a boreal-type forest ecosystem shaped
718 by fire, similar to those of Washington, British Columbia, Northwest Territories, Yukon and Alaska (but see Sect.
719 4.3).

720 4 DISCUSSION

721 4.1 Geochronology

722 The plant and animal fossil assemblages observed at BP suggest a depositional age between 3 and 5 Ma (Matthews Jr
723 and Oviden, 1990; Tedford and Harington, 2003). This biostratigraphic age was corroborated with an amino-acid
724 racemization age ($>2.4 \pm 0.5$ Ma) and Sr-correlation age (2.8–5.1 Ma) on shells (Brigham-Grette and Carter, 1992) in
725 biostratigraphically correlated sediments on Meighen Island, situated 375 km to the west-north-west. The previously
726 calculated burial age of 3.4 Ma for the BP site is a minimum age because no post-depositional production of ^{26}Al or
727 ^{10}Be by muons was assumed. If the samples are considered to have been buried at only the current depth (ca. 10 m,
728 see supplemental data) then the ages plot to the left and outside of the burial field, indicating that the burial depth was
729 significantly deeper for most of the post-depositional history. The revised cosmogenic nuclide burial age is $3.9 \pm 1.5/-$
730 0.5 Ma. It is the best interpretation of burial age data based on improved production rate systematics (e.g. Lifton et
731 al., 2014), and more reasonable estimates of erosion rate and ice cover since the mid-Pliocene (see Fig. S3; Table S5).
732 As the stratigraphic position of the cosmogenic samples is very close to the BP peat layers, we interpret the age to
733 represent the approximate time that the peat was deposited.

734 4.2 Fire, vegetation, temperature: a feedback triangle

735 Wildfire is a key driver of ecological processes in modern boreal forests (Flannigan et al., 2009; Ryan, 2002), and
736 although historically rare, is becoming more frequent in the tundra in recent years (Mack et al., 2011). The modern
737 increase in fire frequency is likely as a consequence of atmospheric CO_2 driven climate warming and feedbacks such
738 as reduced sea ice extent (Hu et al., 2010), because the probability of fire is highest where temperature and moisture
739 are conducive to growth and drying of fuels followed by conditions that favor ignition (Whitman et al., 2015). Young
740 et al. (2017) confirmed the importance of summer warmth and moisture availability patterns in predicting fire across
741 Alaska, highlighting a July temperature of $\sim 13.5^\circ\text{C}$ as a key threshold for fire across Alaska.

Deleted: day

Deleted: as

Deleted: 4

Deleted: Pliocene atmospheric CO_2 levels

We have derived a transfer function that allows us to predict the partial pressure of atmospheric CO_2 in Earths' past based on carbon isotopic measurements in bryophytes. However, many of the studies included in our transfer function identify other mechanisms that may also influence carbon isotopic discrimination in bryophytes. Because these other mechanisms may violate the assumptions of applying this transfer function to the past or contribute error to our reconstructions of atmospheric CO_2 concentrations during the Pliocene, we discuss these mechanisms below.

It has been suggested that in the absence of stomatal regulation, that surface water may control the gradient in partial pressure (i.e. p_i/p_a) in bryophytes (White et al., 1994), due to the greater resistance to diffusion of CO_2 in water than in the atmosphere. For instance, M enot and Burns (2001) found that most mosses growing along an elevational transect in Switzerland experienced discrimination with elevation in response to decreased partial pressure, except one species *Sphagnum cuspidatum* Ehrh. ex Hoffm., which grows almost exclusively in wet hollows. In a study of Hawaiian bryophytes Waite and Sack (2011) found consistent slopes of less isotopic discrimination with elevation in all species, however, species growing on young substrate showed significantly less isotopic discrimination. The most likely explanation is that lack of canopy cover on the older substrates lead to greater photosynthetic rates, which lead to reduced p_i . Lastly, decreased discrimination of mosses growing along an elevational transect in Poland (Skrzypek et al., 2007), was found to be highly correlated with temperature. Although temperature is the primary factor driving most metabolic reactions, it does not provide a physical mechanism explaining the relationship between elevation and isotopic discrimination in mosses. Skrzypek et al. (2007) found slightly different relationships between elevation and carbon isotopic discrimination in mosses growing on the windward versus leeward side of their elevational transects suggesting that changes in lapse rate may also play a factor. Collectively, these studies suggest that microclimatic factors may explain differences in isotopic discrimination of mosses within and among different sites possibly contributing to different intercepts for sites reported in Fig. 3, and that dry vs. moist lapse rates may also play a role in regulating the different slopes among sites. In fact, the greatest elevational range reported among sites was for the elevational transect in the Andes (320 to 3100 m), but this site did not experience the widest range in $\Delta^{13}\text{C}_{\text{moss}}$. This tropical transect had a very moist lapse rate resulting in the least change in atmospheric temperature and humidity with elevation. Nonetheless, by projecting these data as a function of partial pressure we provide a physical mechanism to explain variations in moss carbon isotopic values globally and we help reconcile the previously reported empirical relationships, such as elevation, temperature, and over-story, all of which tend to be covariates of decreasing partial pressure with elevation. While differences in microclimate and lapse rate are clearly important factors in regulating $\Delta^{13}\text{C}_{\text{moss}}$, these factors contribute to the global error in our model for predicting p_a and ultimately to uncertainties in our estimates of atmospheric CO_2 concentrations during the Pliocene.

Our reconstructions of CO_2 concentration for this mid-Pliocene interval are within the range of previously reported CO_2 estimates, tending to agree with alkenone estimates from Pagani et al. (2010). This suggests that CO_2 concentrations during this warm Pliocene interval were above 400 ppm. In fact, our mean Pliocene value (410 ± 50 ppm) is not statistically different from the alkenone based estimates (357 ± 47 ppm) previously reported.

Deleted: climate

896 The abundance of charcoal at BP demonstrates that climatic conditions were conducive to ignition and that sufficient
897 biomass available for combustion existed across the landscape. brGDGTs-derived temperature estimates suggest mean
898 summer temperatures at BP exceeded the ~13.5 °C threshold (Young et al., 2017) that drastically increases the chance
899 of wildfire. Indeed, the estimate of ~15.4°C suggests summer temperatures is ~11°C higher than modern day Eureka,
900 Canada (~4.1°C; Fig. 2). Given a global mean increase of 3°C for the Pliocene compared to modern (see fig. 1) this
901 11°C increase represents 3.6x arctic amplification of temperature (NB. although comparing summer temperatures to
902 mean global temperature increase is likely imprecise, given much increase of arctic warmth in Pliocene climate models
903 is from winter warming (see Ballantyne et al. 2013) 3.6x is likely an underestimate rather than an overestimate.)
904 Without increasing arctic amplification of temperature that accompanies increasing CO₂, mean summer temperatures
905 would fall below the ~13.5°C threshold. This is evidence that Pliocene arctic amplification of temperatures was a
906 direct feedback to increased wildfire activity, but also an indirect feedback as the increased extent of boreal forest into
907 the higher latitudes, also possible due to arctic amplification of temperatures, provided the fuel (Fig. 6)

908 An increase in atmospheric convection has been simulated in response to diminished sea-ice during warmer intervals
909 (Abbot and Tziperman, 2008), but this study did not confirm if this increase in atmospheric convection was sufficient
910 to cause lightning ignitions. An alternative ignition source for combustion of biomass on Ellesmere Island during the
911 Pliocene is coal seam fires, which have been documented to be burning at this time (Estrada et al., 2009). However,
912 given the interaction of summer warmth and ignition by lightning within the same climate range as posited for BP, we
913 consider lightning the most likely source of ignition for Pliocene fires in the High Arctic.

914 Fire return intervals cannot be calculated from the BP charcoal counts due to the absence of a satisfactory age-depth
915 model and discontinuous sampling. As strong interactions are observed between fire regime and ecosystem
916 assemblage in the boreal forest (Brown and Giesecke, 2014; Kasischke and Turetsky, 2006), and in response to
917 climate, comparison with modern fire regimes for areas with shared species compositions and climates may inform a
918 potential range of mean fire return interval (MFR).

919 Matthews and Fyles (2000) indicated that the Pliocene BP environment was characterized by an open larch
920 dominated forest-tundra environment, sharing most species in common with those now found in three regions,
921 including central Alaska to Washington in western North America, the region centered around the Canadian/US border
922 in eastern North America, as well as Fennoscandia in Europe. The modern area with the most species in common with
923 BP is central northern Alaska (Fig. 7A). The area over which shared species were calculated is largely tundra, but
924 includes the ecotone between tundra and boreal forest. Other zones that share many species with BP are continuous
925 with Alaska down the western coast of North America to the region around the border of Canada and the United States,
926 the eastern coast of North America in the region around the border of Canada and the United States (~50°N), and
927 central Fennoscandia. Of these zones, the MST of Alaskan tundra sites (6–9°C) are less similar to BP (15.4°C) than
928 ~50°N on both western and eastern coastal North American sites and central Fennoscandia (12–18°C, Fig. 7B). The
929 eastern coast of North America has higher rainfall during the summer (>270 mm), than the west coast and Alaska
930 (Fig. 7C), which correlates to the timing of western fires. The low summer precipitation for much of the west (<200
931 mm), is consistent with previously published summer precipitation estimates for BP (~190 mm). As a result, the fire
932 regime of the west coast ~50°N may be a better analogue for BP than the east coast of North America. In central

Deleted: r

Deleted: r

Formatted: Not Highlight

935 Fennoscandia there is also a west vs. east coastal variation in summer precipitation with the western, Nordic part of
936 the region experiencing higher summer precipitation (252– >288 mm), than the more similar eastern, Swedish part of
937 the region (~198 mm).

938 Investigation of the modern fire detection data (Fig. 7D) suggests that the two regions most climatically similar to
939 BP, ~50°N western North America and central Sweden, have radically different fire regimes. It is likely this is caused
940 by historical fire suppression in Sweden that limits the utility of modern data for comparison with this study (Brown
941 and Giesecke, 2014; Niklasson and Granström, 2004). To understand the fire regimes, as shaped by climate and species
942 composition rather than human impacts, we considered both the modern and recent Holocene reconstructions for these
943 regions (Table 1). This shows that, a) within any region variation arises from the complex spatial patterning of fire
944 across landscapes, and b) that the regions most similar to BP (~50°N western North American and eastern
945 Fennoscandian reconstructions for the recent Holocene) have shorter fire return intervals than the cooler Alaskan
946 tundra or wetter summer ~50°N region of the eastern North American coast.

947 While the shared species for Siberia appears low, the number of observations in the modern biodiversity database
948 used is likewise low – perhaps causatively so. Given the similar climate to BP on the Central Siberian Plateau and
949 some key aspects of the floras in Siberia such as the dominance of larch, we considered the fire regime of the larch
950 forests of Siberia. Kharuk et al. (2016; 2011) studied MFRI across Siberia, from 64°N to 71°N, the northern limit of
951 larch stands. They found an average MFRI across that range of 110 years, with MFRI increasing from 80 years in the
952 southern latitudes to ~300 in the north (Table 1). Based on similarity of the climate variables, the more southerly
953 MFRI (~80 years) may be a better analogue. Key differences between boreal fires in North America compared to
954 Russia are a higher fire frequency with more burned area in Russia, but a much lower crown fire and a difference in
955 timing of disturbance, with spring fires prevailing in Russia compared to mid-summer fires in western Canada (de
956 Groot et al., 2013; Rogers et al., 2015).

957 The pollen-based vegetation reconstruction derived in this study indicates that open *Larix-Betula* parkland persisted
958 in the basal (380.3–380.4 MASL) parts of the sequence. Groundcover was additionally dominated by shrub birch,
959 ericaceous heath and ferns. While the regional climate may have been somewhat dry, the record suggests that, locally,
960 a moist fen environment dominated by Cyperaceae, existed near the sampling location. Shrubs including *Alnus* and
961 *Salix* likely occupied the wetland margins.

962 The corresponding relatively low concentration of charcoal may reflect lower severity fires or higher sedimentation
963 rates. We consider the former more likely due to the depositional environment of Unit III from Mitchell et al. 2016, a
964 lake edge fen peat in a beaver pond or small lake, without evidence of high sediment influx overwhelming peat
965 production. We posit that a surface fire regime, somewhat like that in southern central Siberia existed. This premise
966 is also supported by the fire ecology characteristics of the dominant vegetation. *Larix* does not support crown fires
967 due to leaf moisture content (de Groot et al., 2013) and self-pruning (Kobayashi et al., 2007). The persistence and
968 success of larch in modern-day Siberia appears to be driven by its high growth rate (Jacquelyn et al., 2017) tolerance
969 of frequent surface fire due to thick lower bark (Kobayashi et al., 2007) and tolerance of spring drought due to its
970 deciduous habit (Berg and Chapin III, 1994). Arboreal *Betula* are very intolerant of fire and easily girdled. However,
971 they are quick to resprout and are often found in areas with short fire return intervals. Like *Larix*, arboreal *Betula* have

Deleted: Comparison to m

Deleted: This is likely

Deleted: very

Deleted: in

Deleted: the

Deleted: 0

Deleted: 0

Deleted: If the former, it is posited

980 high moisture content of their foliage and are not prone to crown fires. *Betula nana* L., an extant dwarf birch, is a fire
981 endurer that resprouts from underground rhizomes or roots (Racine et al., 1987) thus regenerating quickly following
982 lower severity fires (de Groot et al., 1997). The vegetation and fire regime characteristics are similar further up the
983 sequence at 381.10-381.25 MASL, with the exception that ferns increased in abundance while heath decreased.

984 In the upper part of the sequence (381.35-381.45 MASL), where charcoal was abundant, the *Larix-Betula* parkland
985 was replaced by a mixed boreal forest assemblage with a fern understory. Canopy cover was more closed compared
986 to the preceding intervals. The forest was dominated by *Larix* and *Picea*, with lesser amounts of *Pinus*. While *Betula*
987 remained part of the forest, it decreased in abundance possibly due to increased competition with the conifers. Based
988 on exploratory CRACLE analyses of climate preferences using GBIF occurrence data (GBIF.org, 2018a, b, c, d) of
989 the dominant taxa (*Larix-Betula* vs. *Larix-Picea-Pinus*), the expansion of conifers could indicate slightly warmer
990 summers (MST ~15.8 °C vs. 17.1 °C). This result differs from the stable MST estimated by bacterial tetraethers,
991 although within reported error, and the small change is certainly within the climate distributions of both communities.
992 The CRACLE analyses also suggest that slightly drier conditions may have prevailed during the three wettest months
993 (249-285mm vs. 192-219mm). While the interaction between climate, vegetation and fire is complex, small changes
994 in MST and precipitation could have directly altered both the vegetation and fire regime, which in turn further
995 promoted fire adapted taxa. In addition to regional climatic factors, community change at the site may have been
996 further influenced by local hydrological conditions, such as channel migration, pond infilling and ecosystem
997 engineering by beaver (*Cantor spp.*).

998 The high charcoal content of the upper portion (~ Unit IV) of the sequence has three potential explanations:
999 reworking of previously deposited charcoal, decreased sedimentation, or increased wildfire production of charcoal.
1000 We consider the first unlikely because there is no difference in the shape of the macrocharcoal between the upper and
1001 lower portions of the sequence, whereas we would anticipate a change in the dimensions of the charcoal if it had
1002 undergone additional physical breakdown from reworking (see Fig. S4). The second, decreased sedimentation, may
1003 occur if the deposition is a result of infrequent, episodic flooding intermixed with long periods during which charcoal
1004 was deposited. The recorded sedimentology does not support this explanation, but due to the complexity of flooding
1005 processes, also does not disprove this explanation. We, however, favour the third explanation of increased wildfire
1006 due to the change in plant composition consistent with a greater influence of fire. If accepted, it is likely that frequent,
1007 mixed severity fires persisted. While *Larix* is associated with surface fire, *Picea* and *Pinus* are adapted to higher
1008 intensity crown fires. A crown fire regime may have established as conifers expanded, altering fuel loads and
1009 flammability. For example, black spruce sheds highly flammable needles, its lower branches can act as fuel ladders
1010 facilitating crown fires (Kasischke et al., 2008), and it was previously tentatively identified at BP (Fletcher et al.,
1011 2017). While it has thin bark and shallow roots maladapted to survive fire (Auclair, 1985; Brown, 2008; Kasischke et
1012 al., 2008), it releases large numbers of seeds from semi-serotinous cones, leading to rapid re-establishment (Côté et
1013 al., 2003). The documentation of Onagraceae pollen at the top of the sequence could potentially reflect post-fire
1014 succession. For example, the species *Epilobium angustifolium* L. is an early-seral colonizer of disturbed (i.e. burned)
1015 sites, pollinated by insects.

Deleted: 0

Deleted: 0

Deleted: 0

Deleted: 0

Deleted: e

Deleted: s

Deleted: 5

Deleted: If excepted

Deleted: t

1025 It appears that the *Larix-Betula* parkland dominated intervals correspond to the peat- and sand-stratigraphic Units II
1026 and III described by Mitchell et al. (2016), whereas the mixed boreal forest in the upper part of the sequence is
1027 contemporaneous with Unit IV, described as peat and peaty sand, coarsening upwards. While it is clear that the
1028 vegetation and fire regimes changed through time at this Arctic site, temperatures appear more stable, or at least to
1029 have no apparent trend. Thus, it is suggested that the fire regime at BP was primarily regulated by regional climate
1030 and vegetation, and perhaps additionally by changing local hydrological conditions. Regarding climate, MST
1031 remained high enough ($> \sim 13.5^{\circ}\text{C}$) throughout the sequence to allow for fire disturbance and the pollen suggests that
1032 temperatures may have marginally increased in the upper part of the sequence. Alternatively, other climate variables,
1033 such as the precipitation regime, or local hydrological change may have initiated the change in community. Up-
1034 sequence changes in vegetation undoubtedly influenced fine fuel loads and flammability. Indeed, the fire ecological
1035 characteristics of the vegetation are consistent with a regional surface fire regime yielding to a crown fire regime.

1036 *Betula* and *Alnus*, which occurred earlier in the depositional sequence, are favored by beaver in foraging (Busher,
1037 1996; Haarberg and Rosell, 2006; Jenkins, 1979). Moreover, the presence of sticks cut by beaver in Unit III reveals
1038 that beavers were indeed at the site, moistening the local land surface. The lack of beaver cut sticks and changes in
1039 sediment in Unit IV may indicate that the beavers abandoned the site, possibly in response to changes in vegetation
1040 (i.e. increased conifers and decreased *Betula*) limiting preferred forage or due to lateral channel migration, as
1041 evidenced by the coarsening upward sequence described by Mitchell et al. (2016). As a result, the local land surface
1042 may have become somewhat drier, contemporaneous with the change towards *Larix-Picea-Pinus* forest and a mixed
1043 severity fire regime.

1044 Critically, the charcoal record at BP suggests substantial biomass burning that could have acted as a feedback
1045 mechanism amplifying or dampening warming during the Pliocene. Its potential role as a feedback to climate is
1046 suggested by its prevalence through time, and forest fire's complex direct impacts on the surface radiative budget (e.g.
1047 black carbon deposition on snow and ice) and direct and indirect effects on the top of the atmosphere radiative budget
1048 (i.e. aerosol emissions; Feng et al., 2016). Further investigation through both investigation of the fire record at other
1049 Arctic sites and modelling experiments using varying fire regimes and extent is warranted to better characterize the
1050 fire regime in order to improve accuracy of fire simulations in earth system models of Pliocene climate.

1051 5. CONCLUSION

1052 The novel temperature estimates presented here confirm that summer temperatures were considerably warmer during
1053 the Pliocene ($15.4 \pm 0.8^{\circ}\text{C}$) compared to the modern Arctic. The $\sim 11^{\circ}\text{C}$ higher summer temperatures at Beaver Pond
1054 support an increasing influence of arctic amplification of temperatures when CO_2 reaches and exceeds modern levels.
1055 Our reconstruction of the paleovegetation and ecology of this unique site on Ellesmere Island suggests an assemblage
1056 similar to forests of the western margins of North America and eastern Fennoscandia. The evidence of recurrent fire
1057 and concurrent changes in taxonomic composition are indicators that fire played an active role as a feedback in
1058 Pliocene Arctic forests, shaping the environment as it does in the boreal forest today. Evidence from fire in the modern
1059 boreal forest suggests that fire may have had direct and indirect impacts on Earth's radiative budget at high latitudes
1060 during the Pliocene, acting as a feedback to Pliocene climate. The net impact of the component process remains

Deleted: CO₂ and

Deleted: that there was

Deleted: been

Deleted: due to

Deleted: the

Deleted:

Deleted:

Deleted: The record of CO₂ in keeping with upper estimates from the Pliocene supports the hypothesis that Pliocene Arctic terrestrial fossil localities probably represent periods of higher warmth that supported higher productivity.

Deleted: suggest

Deleted: ~

Deleted: day

Deleted:

Deleted: Eureka, Canada (-4.1°C ; Fig. 2)

Deleted: is

Deleted: s

Deleted: as

Deleted: suggests

1081 unknown and modelling experiments are needed to quantitatively investigate the effects of the kind of fire regime
1082 presented here, on the Pliocene High Arctic. Collectively, these reconstructions provide new insights into the
1083 paleoclimatology and paleoecology of the Canadian High Arctic, ~3.9 Ma.

1084

1085 *Data Availability.* The data generated and used in this analysis are available in the supplemental information associated
1086 with this article.

1087

1088 *Sample Availability.* Samples used in this analysis are curated by the Canadian Museum of Nature. Sample numbers
1089 used for each analysis are given in the supplemental information (Table S3 and S4).

1090

1091 *Supplemental Link.* To be provided by Copernicus Publishing

1092

1093 *Author Contribution.* Conceptualization: A.P.B. with modification by other authors; Methodology: J.G., J.S.S.D.,
1094 K.J.B., T.F.; Formal analysis: All authors; Investigation: A.P.B., J.G., K.J.B., L.W., T.F.; Resources: A.P.B., J.G.,
1095 J.S.S.D., K.J.B.; Data curation: A.P.B., J.G., K.J.B., L.W., T.F.; Writing—Original draft: All authors; Writing—
1096 Review and editing: All authors; Supervision: A.P.B., J.S.S.D., K.J.B., N.R.; Project administration: A.P.B., N.R.,
1097 T.F.; Funding acquisition: A.P.B., J.G., J.S.S.D., K.J.B., N.R., T.F. (Definitions as per the CRediT Taxonomy)

1098

1099 *Competing interests.* The authors declare that they have no conflict of interest

1100

1101 *Acknowledgements.* This work was funded by NSF Polar Programs to A.P.B.; National Geographic Committee for
1102 Research and Exploration Grant (9912-16) and Endeavour Research Fellowship (5928-2017) to T.F.; National
1103 Geographic Explorer Grant (7902-05), NSERC Discovery Grant (312193), and The W. Garfield Weston Foundation
1104 grant to N.R.; student travel (N.R. supervised) was supported by the Northern Scientific Training Program (NSTP)
1105 from the government of Canada; an NSERC Discovery Grant (239961) with Northern Supplement (362148) to J.C.G.;
1106 Natural Resources Canada (SO-03 PA 3.1 Forest Disturbances Wildland Fire) to K.J.B.; the European Research
1107 Council under the European Union's Seventh Framework Programme (FP7/2007-2013) / ERC grant agreement n^o
1108 [226600], and funding from the Netherlands Earth System Science Center (NESSC) through a gravitation grant (NWO
1109 024.002.001) from the Dutch Ministry for Education, Culture and Science to J.S.S.D.

1110 We are also grateful to Nicholas Conder (Canadian Forest Service) who assisted with sample preparation for the
1111 vegetation/fire reconstruction. We also acknowledge the 2006, 2008, 2010 and 2012 field teams including D. Finney
1112 (Environment Canada), H. Larson (McGill University), M. Vavrek (McGill University), A. Dececchi (McGill
1113 University), W.T. Mitchell (Carleton University), R. Smith (University of Saskatchewan), and C. Schröder-Adams
1114 (Carleton University). The field research was supported by a paleontology permit from the Government of Nunavut,
1115 CLEY (D.R. Stenton, J. Ross) and with the permission of Qikiqtani Inuit Association, especially Grise Fiord
1116 (Nunavut). Logistic support was provided by the Polar Continental Shelf Program (M. Bergmann, B. Hycryk, B.
1117 Hough, M. Kristjanson, T. McConaghy, J. MacGregor and the PCSP team).

Deleted: A.P.B.,

Deleted: Alice Telka (Paleotec Services) identified and prepared macrofossil plants for the CO₂ analysis

1121 **References**

- 1122 Abbot, D. S. and Tziperman, E.: Sea ice, high-latitude convection, and equable climates, *Geophysical Research*
1123 *Letters*, 35, 2008.
- 1124 Auclair, A. N.: Postfire regeneration of plant and soil organic pools in a *Picea mariana*–*Cladonia stellaris* ecosystem,
1125 *Canadian Journal of Forest Research*, 15, 279–291, 1985.
- 1126 Ballantyne, A. P., Axford, Y., Miller, G. H., Otto-Bliesner, B. L., Rosenbloom, N., and White, J. W.: The amplification
1127 of Arctic terrestrial surface temperatures by reduced sea-ice extent during the Pliocene, *Palaeogeography,*
1128 *Palaeoclimatology, Palaeoecology*, 386, 59–67, 2013.
- 1129 Ballantyne, A. P., Greenwood, D. R., Sinnighe Damsté, J. S., Csank, A. Z., Eberle, J. J., and Rycbizynski, N.:
1130 Significantly warmer Arctic surface temperatures during the Pliocene indicated by multiple independent proxies,
1131 *Geology*, 38, 603–606, 2010.
- 1132 Ballantyne, A. P., Rycbizynski, N., Baker, P. A., Harington, C. R., and White, D.: Pliocene Arctic temperature
1133 constraints from the growth rings and isotopic composition of fossil larch, *Palaeogeography, Palaeoclimatology,*
1134 *Palaeoecology*, 242, 188–200, 2006.
- 1135 Bendle, J. A., Weijers, J. W., Maslin, M. A., Sinnighe Damsté, J. S., Schouten, S., Hopmans, E. C., Boot, C. S., and
1136 Pancost, R. D.: Major changes in glacial and Holocene terrestrial temperatures and sources of organic carbon recorded
1137 in the Amazon fan by tetraether lipids, *Geochemistry, Geophysics, Geosystems*, 11, 2010.
- 1138 Berg, E. E. and Chapin III, F. S.: Needle loss as a mechanism of winter drought avoidance in boreal conifers, *Canadian*
1139 *Journal of Forest Research*, 24, 1144–1148, 1994.
- 1140 Bergeron, Y.: The influence of island and mainland lakeshore landscapes on boreal forest fire regimes, *Ecology*, 72,
1141 1980–1992, 1991.
- 1142 Bergeron, Y., Cyr, D., Drever, C. R., Flannigan, M., Gauthier, S., Kneeshaw, D., Lauzon, È., Leduc, A., Goff, H. L.,
1143 Lesieur, D., and Logan, K.: Past, current, and future fire frequencies in Quebec's commercial forests: implications for
1144 the cumulative effects of harvesting and fire on age-class structure and natural disturbance-based management,
1145 *Canadian Journal of Forest Research*, 36, 2737–2744, 2006.
- 1146 Bouchard, M., Pothier, D., and Gauthier, S.: Fire return intervals and tree species succession in the North Shore region
1147 of eastern Quebec, *Canadian Journal of Forest Research*, 38, 1621–1633, 2008.
- 1148 Brigham-Grette, J. and Carter, L. D.: Pliocene Marine Transgressions of Northern Alaska: Circumarctic Correlations
1149 and Paleoclimatic Interpretations, *Arctic*, 45, 74–89, 1992.
- 1150 Brown, K. J. and Giesecke, T.: Holocene fire disturbance in the boreal forest of central Sweden, *Boreas*, 43, 639–651,
1151 2014.
- 1152 Brown, K. J. and Power, M. J.: Charred particle analyses. In: *Encyclopedia of Quaternary Science*, Elias, S. (Ed.),
1153 Elsevier, Amsterdam, 2013.
- 1154 Brown, M.: Fire and Ice: Fire Severity and Future Flammability in Alaskan Black Spruce Forests, *Fire Science Brief*,
1155 2008. 1–6, 2008.
- 1156 [Bush, E. and Lemmen, D.S.\(eds\): Canada's Changing Climate Report; Government of Canada, Ottawa, ON. 444 p.,](#)
1157 [2019](#)

Deleted: Bauska, T. K., Bagginstos, D., Brook, E. J., Mix, A. C., Marcott, S. A., Petrenko, V. V., Schaefer, H., Severinghaus, J. P., and Lee, J. E.: Carbon isotopes characterize rapid changes in atmospheric carbon dioxide during the last deglaciation, *Proceedings of the National Academy of Sciences*, 2016. 201513868, 2016.*

Deleted: Bonan, G.: *Ecological climatology: concepts and applications*, Cambridge University Press, 2015.*

1165 Busher, P. E.: Food Caching Behavior of Beavers (*Castor canadensis*): Selection and Use of Woody Species, The
 1166 American Midland Naturalist, 135, 343-348, 1996.

1167 Clymo, R. S.: The Origin of Acidity in Sphagnum Bogs, The Bryologist, 67, 427-431, 1964.

1168 Côté, M., Ferron, J., and Gagnon, R.: Impact of seed and seedling predation by small rodents on early regeneration
 1169 establishment of black spruce, Canadian Journal of Forest Research, 33, 2362-2371, 2003.

1170 Csank, A. Z., Patterson, W. P., Eglinton, B. M., Rybczynski, N., and Basinger, J. F.: Climate variability in the Early
 1171 Pliocene Arctic: Annually resolved evidence from stable isotope values of sub-fossil wood, Ellesmere Island, Canada,
 1172 Palaeogeography, Palaeoclimatology, Palaeoecology, 308, 339-349, 2011a.

1173 Csank, A. Z., Tripathi, A. K., Patterson, W. P., Eagle, R. A., Rybczynski, N., Ballantyne, A. P., and Eiler, J. M.:
 1174 Estimates of Arctic land surface temperatures during the early Pliocene from two novel proxies, Earth and Planetary
 1175 Science Letters, 304, 291-299, 2011b.

1176 de Groot, W. J., Cantin, A. S., Flannigan, M. D., Soja, A. J., Gowman, L. M., and Newbery, A.: A comparison of
 1177 Canadian and Russian boreal forest fire regimes, Forest Ecology and Management, 294, 23-34, 2013.

1178 de Groot, W. J., Thomas, P. A., and Wein, R. W.: *Betula nana* L. and *Betula glandulosa* Michx, Journal of Ecology,
 1179 85, 241-264, 1997.

1180 De Jonge, C., Hopmans, E. C., Stadnitskaia, A., Rijpstra, W. I. C., Hofland, R., Tegelaar, E., and Sinninghe Damsté,
 1181 J. S.: Identification of novel penta- and hexamethylated branched glycerol dialkyl glycerol tetraethers in peat using
 1182 HPLC-MS 2, GC-MS and GC-SMB-MS, Organic geochemistry, 54, 78-82, 2013.

1183 De Jonge, C., Hopmans, E. C., Zell, C. I., Kim, J.-H., Schouten, S., and Sinninghe Damsté, J. S.: Occurrence and
 1184 abundance of 6-methyl branched glycerol dialkyl glycerol tetraethers in soils: Implications for palaeoclimate
 1185 reconstruction, Geochimica et Cosmochimica Acta, 141, 97-112, 2014.

1186 De Jonge, C., Stadnitskaia, A., Hopmans, E. C., Cherkashov, G., Fedotov, A., Streletskaia, I. D., Vasiliev, A. A., and
 1187 Sinninghe Damsté, J. S.: Drastic changes in the distribution of branched tetraether lipids in suspended matter and
 1188 sediments from the Yenisei River and Kara Sea (Siberia): Implications for the use of brGDGT-based proxies in coastal
 1189 marine sediments, Geochimica et Cosmochimica Acta, 165, 200-225, 2015.

1190 de Lafontaine, G. and Payette, S.: Shifting zonal patterns of the southern boreal forest in eastern Canada associated
 1191 with changing fire regime during the Holocene, Quaternary Science Reviews, 30, 867-875, 2011.

1192 Dowsett, H., Dolan, A., Rowley, D., Pound, M., Salzmann, U., Robinson, M., Chandler, M., Foley, K., and Haywood,
 1193 A.: The PRISM4 (mid-Piacenzian) palaeoenvironmental reconstruction, Climate of the Past, doi:doi:10.5194/cp-12-
 1194 1519-2016, 2016. 2016.

1195 Dowsett, H. J., Cronin, T. M., Poore, R. Z., Thompson, R. S., Whatley, R. C., and Wood, A. M.: Micropaleontological
 1196 evidence for increased meridional heat transport in the North Atlantic Ocean during the Pliocene, Science, 258, 1133-
 1197 1136, 1992.

1198 Dowsett, H. J., Robinson, M. M., Haywood, A. M., Hill, D. J., Dolan, A. M., Stoll, D. K., Chan, W. L., Abe-Ouchi,
 1199 A., Chandler, M. A., and Rosenbloom, N. A.: Assessing confidence in Pliocene sea surface temperatures to evaluate
 1200 predictive models, Nature Climate Change, 2, 365-371, 2012.

Deleted: Dee, D. P., Uppala, S. M., Simmons, A. J., Berrisford, P., Poli, P., Kobayashi, S., Andrae, U., Balmaseda, M. A., Balsamo, G., and Bauer, P.: The ERA-Interim reanalysis: Configuration and performance of the data assimilation system, Quarterly Journal of the Royal Meteorological Society, 137, 553-597, 2011. [Diefendorf, A. F., Mueller, K. E., Wing, S. L., Koch, P. L. and Freeman, K. H.: Global patterns in leaf 13C discrimination and implications for studies of past and future climate. Proceedings of the National Academy of Sciences, 107, 5738-5743, 2010.](#)

1210 Estrada, S., Piepjohn, K., Frey, M. J., Reinhardt, L., Andruleit, H., and von Gosen, W.: Pliocene coal-seam fires on
 1211 southern Ellesmere Island, Canadian Arctic, Neues Jahrbuch für Geologie und Paläontologie - Abhandlungen, 251,
 1212 33-52, 2009.

1213 ~~Feng, R., Otto-Bliesner, B., Fletcher, T., Ballantyne, A., and Brady, E.: Contributions to Pliocene Arctic warmth from
 1214 removal of anthropogenic aerosol and enhanced forest fire emissions, San Francisco, USA. 2016, PP33A-2344.~~
 1215 Feng, R., Otto-Bliesner, B. L., Fletcher, T. L., Tabor, C. R., Ballantyne, A. P., and Brady, E. C.: Amplified Late
 1216 Pliocene terrestrial warmth in northern high latitudes from greater radiative forcing and closed Arctic Ocean gateways,
 1217 Earth and Planetary Science Letters, 466, 129-138, 2017.

1218 Flannigan, M., Stocks, B., Turetsky, M., and Wotton, M.: Impacts of climate change on fire activity and fire
 1219 management in the circumboreal forest, Global Change Biology, 15, 549–560, 2009.

1220 ~~Fletcher, T., Feng, R., Telka, A. M., Matthews, J. V., and Ballantyne, A.: Floral dissimilarity and the influence of
 1221 climate in the Pliocene High Arctic: Biotic and abiotic influences on five sites on the Canadian Arctic Archipelago,
 1222 Frontiers in Ecology and Evolution, 5, 19, 2017.~~

1223 Foster, L. C., Pearson, E. J., Juggins, S., Hodgson, D. A., Saunders, K. M., Verleyen, E., and Roberts, S. J.:
 1224 Development of a regional glycerol dialkyl glycerol tetraether (GDGT)–temperature calibration for Antarctic and sub-
 1225 Antarctic lakes, Earth and Planetary Science Letters, 433, 370–379, 2016.

1226 ~~Francis, J. and Skific, N.: Evidence linking rapid Arctic warming to mid-latitude weather patterns, Philosophical
 1227 Transactions of the Royal Society A: Mathematical, Physical and Engineering Sciences, 373, 1–12, 2015.~~

1228 GBIF.org: GBIF Occurrence Download (Beaver Pond extant species) <http://doi.org/10.15468/dl.ertiqj> 1st February
 1229 2017.

1230 GBIF.org: GBIF Occurrence Download (*Betula*) <https://doi.org/10.15468/dl.akxgp5> 11th May 2018a.

1231 GBIF.org: GBIF Occurrence Download (*Larix*) <https://doi.org/10.15468/dl.mfhnci> 11th May 2018b.

1232 GBIF.org: GBIF Occurrence Download (*Picea*) <https://doi.org/10.15468/dl.wi7jdc> 11th May 2018c.

1233 GBIF.org: GBIF Occurrence Download (*Pinus*) <https://doi.org/10.15468/dl.vwfjj2> 11th May 2018d.

1234 ~~Greene, G. A. and Daniels, L. D.: Spatial interpolation and mean fire interval analyses quantify historical mixed-
 1235 severity fire regimes, International Journal of Wildland Fire, 26, 136–147, 2017.~~

1236 Haarberg, O. and Rosell, F.: Selective foraging on woody plant species by the Eurasian beaver (*Castor fiber*) in
 1237 Telemark, Norway, Journal of Zoology, 270, 201-208, 2006.

1238 Haywood, A. M., Dowsett, H. J., and Dolan, A. M.: Integrating geological archives and climate models for the mid-
 1239 Pliocene warm period, Nature communications, 7, 1-14, 2016.

1240 Higuera, P., Barnes, J. L., Chipman, M. L., Urban, M., and Hu, F. S.: The burning tundra: A look back at the last 6,000
 1241 years of fire in the Noatak National Preserve, Northwestern Alaska, Alaska Park Science, 10, 37–41, 2011.

1242 Higuera, P. E., Brubaker, L. B., Anderson, P. M., Hu, F. S., and Brown, T. A.: Vegetation mediated the impacts of
 1243 postglacial climate change on fire regimes in the south-central Brooks Range, Alaska, Ecological Monographs, 79,
 1244 201–219, 2009.

1245 Hijmans, R. J., Cameron, S. E., Parra, J. L., Jones, P. G., and Jarvis, A.: Very high resolution interpolated climate
 1246 surfaces for global land areas, International Journal of Climatology, 25, 1965–1978, 2005.

Deleted: Farquhar, G. D., Ehleringer, J. R., and Hubick, K. T.: Carbon isotope discrimination and photosynthesis, Annual Review of Plant Biology, 40, 503–537, 1989.¶

Deleted: Fletcher, B. J., Brentnall, S. J., Anderson, C. W., Berner, R. A., and Beerling, D. J.: Atmospheric carbon dioxide linked with Mesozoic and early Cenozoic climate change, Nature Geoscience, 1, 43–48, 2008.¶

Deleted: Foster, G. L., Royer, D. L., and Lunt, D. J.: Future climate forcing potentially without precedent in the last 420 million years, Nature Communications, 8, 14845, 2017.¶

Deleted: Global View-CO₂: Cooperative Global Atmospheric Data Integration Project. 2013, updated annually. Multi-laboratory compilation of synchronized and gap-filled atmospheric carbon dioxide records for the period 1979-2012. Compiled by NOAA Global Monitoring Division: Boulder, Colorado, U.S.A. 2013.¶

1262 ~~Hopmans, E. C., Schouten, S., and Sinninghe Damsté, J. S.: The effect of improved chromatography on GDGT-based~~
1263 ~~palaeoproxies, *Organic Geochemistry*, 93, 1–6, 2016.~~

1264 Hu, F. S., Higuera, P. E., Walsh, J. E., Chapman, W. L., Duffy, P. A., Brubaker, L. B., and Chipman, M. L.: Tundra
1265 burning in Alaska: Linkages to climatic change and sea ice retreat, *Journal of Geophysical Research: Biogeosciences*,
1266 115, 2010.

1267 ~~Huguet, C., Hopmans, E. C., Febo-Ayala, W., Thompson, D. H., Sinninghe Damsté, J. S., and Schouten, S.: An~~
1268 ~~improved method to determine the absolute abundance of glycerol dibiphytanyl glycerol tetraether lipids, *Organic*~~
1269 ~~*Geochemistry*, 37, 1036–1041, 2006.~~

1270 Hwang, Y. T., Frierson, D. M., and Kay, J. E.: Coupling between Arctic feedbacks and changes in poleward energy
1271 transport, *Geophysical Research Letters*, 38, 2011.

1272 Jacquelyn, K. S., Adrianna, C. F., Herman, H. S., Amanda, H.-H., Alexander, K., Tatiana, L., Dmitry, E., and Elena,
1273 S.: Fire disturbance and climate change: implications for Russian forests, *Environmental Research Letters*, 12, 035003,
1274 2017.

1275 Jenkins, S. H.: Seasonal and year-to-year differences in food selection by beavers, *Oecologia*, 44, 112–116, 1979.

1276 Johnstone, J. F., Chapin, F. S., Hollingsworth, T. N., Mack, M. C., Romanovsky, V., and Turetsky, M.: Fire, climate
1277 change, and forest resilience in interior Alaska, *Canadian Journal of Forest Research*, 40, 1302–1312, 2010a.

1278 Johnstone, J. F., Hollingsworth, T. N., Chapin, F. S., and Mack, M. C.: Changes in fire regime break the legacy lock
1279 on successional trajectories in Alaskan boreal forest, *Global Change Biology*, 16, 1281–1295, 2010b.

1280 Johnstone, J. F. and Kasischke, E. S.: Stand-level effects of soil severity on postfire regeneration in a recently
1281 burned black spruce forest, *Canadian Journal of Forest Research*, 35, 2151–2163, 2005.

1282 Jones, P. D. and Moberg, A.: Hemispheric and large-scale surface air temperature variations: An extensive revision
1283 and an update to 2001, *Journal of Climate*, 16, 206–223, 2003.

1284 Kasischke, E. S. and Turetsky, M. R.: Recent changes in the fire regime across the North American boreal region—
1285 spatial and temporal patterns of burning across Canada and Alaska, *Geophysical research letters*, 33, 2006.

1286 Kasischke, E. S., Turetsky, M. R., Ottmar, R. D., French, N. H., Hoy, E. E., and Kane, E. S.: Evaluation of the
1287 composite burn index for assessing fire severity in Alaskan black spruce forests, *International Journal of Wildland*
1288 *Fire*, 17, 515–526, 2008.

1289 Kasischke, E. S., Williams, D., and Barry, D.: Analysis of the patterns of large fires in the boreal forest region of
1290 Alaska, *International Journal of Wildland Fire*, 11, 131–144, 2002.

1291 Kharuk, V. I., Dvinskaya, M. L., Petrov, I. A., Im, S. T., and Ranson, K. J.: Larch forests of Middle Siberia: long-term
1292 trends in fire return intervals, *Regional Environmental Change*, doi: 10.1007/s10113-016-0964-9, 2016. 1–9, 2016.

1293 Kharuk, V. I., Ranson, K. J., Dvinskaya, M. L., and Im, S. T.: Wildfires in northern Siberian larch dominated
1294 communities, *Environmental Research Letters*, 6, 045208, 2011.

1295 Kobayashi, M., Nemilostiv, Y. P., Zyryanova, O. A., Kajimoto, T., Matsuura, Y., Yoshida, T., Satoh, F., Sasa, K., and
1296 Koike, T.: Regeneration after forest fires in mixed conifer broad-leaved forests of the Amur region in far eastern
1297 Russia: the relationship between species specific traits against fire and recent fire regimes, *Eurasian Journal of Forest*
1298 *Research*, 10, 51–58, 2007.

Deleted: Hönisch, B., Hemming, N. G., Archer, D., Siddall, M., and McManus, J. F.: Atmospheric Carbon Dioxide Concentration Across the Mid-Pleistocene Transition, *Science*, 324, 1551–1554, 2009.[†]

Deleted: Huber, M.: A Hotter Greenhouse?, *Science*, 321, 353–354, 2008.[†]

1305 Kooijman, A. and Westhoff, V.: Variation in habitat factors and species composition of *Scorpidium scorpioides*
1306 communities in NW-Europe, *Plant Ecology*, 117, 133–150, 1995.

1307 Kooijman, A. M. and Paulissen, M. P. C. P.: Higher acidification rates in fens with phosphorus enrichment, *Applied*
1308 *Vegetation Science*, 9, 205–212, 2006.

1309 Lifton, N., Sato, T., and Dunai, T. J.: Scaling in situ cosmogenic nuclide production rates using analytical
1310 approximations to atmospheric cosmic-ray fluxes, *Earth and Planetary Science Letters*, 386, 149–160, 2014.

1311 Lisiecki, L. E. and Raymo, M. E.: A Plio-Pleistocene stack of 57 globally distributed benthic $\delta^{18}\text{O}$ records,
1312 *Paleoceanography*, 20, 2005.

1313 Loomis, S. E., Russell, J. M., Ladd, B., Street-Perrott, F. A., and Sinninghe Damsté, J. S.: Calibration and application
1314 of the branched GDGT temperature proxy on East African lake sediments, *Earth and Planetary Science Letters*, 357,
1315 277–288, 2012.

1316 Lorimer, C. G.: The Presettlement Forest and Natural Disturbance Cycle of Northeastern Maine, *Ecology*, 58, 139–
1317 148, 1977.

1318 Luthi, D., Le Floch, M., Bereiter, B., Blunier, T., Barnola, J.-M., Siegenthaler, U., Raynaud, D., Jouzel, J., Fischer,
1319 H., Kawamura, K., and Stocker, T. F.: High-resolution carbon dioxide concentration record 650,000–800,000 years
1320 before present, *Nature*, 453, 379–382, 2008.

1321 Lynch, J. A., Clark, J. S., Bigelow, N. H., Edwards, M. E., and Finney, B. P.: Geographic and temporal variations in
1322 fire history in boreal ecosystems of Alaska, *Journal of Geophysical Research: Atmospheres*, 107, FFR 8-1–FFR 8-17,
1323 2002.

1324 Mack, M. C., Bret-Harte, M. S., Hollingsworth, T. N., Jandt, R. R., Schuur, E. A. G., Shaver, G. R., and Verbyla, D.
1325 L.: Carbon loss from an unprecedented Arctic tundra wildfire, *Nature*, 475, 489–492, 2011.

1326 Marshall, J., Armour, K. C., Scott, J. R., Kostov, Y., Hausmann, U., Ferreira, D., Shepherd, T. G., and Bitz, C. M.:
1327 The ocean's role in polar climate change: asymmetric Arctic and Antarctic responses to greenhouse gas and ozone
1328 forcing, *Philosophical Transactions of the Royal Society of London A: Mathematical, Physical and Engineering*
1329 *Sciences*, 372, 20130040, 2014.

1330 Matthews Jr, J. V. and Oveden, L. E.: Late Tertiary plant macrofossils from localities in Arctic/sub- Arctic North
1331 America: a review of the data, *Arctic*, 43, 364–392, 1990.

1332 Matthews, J. V. J. and Fyles, J. G.: Late Tertiary plant and arthropod fossils from the High Terrace Sediments on the
1333 Fosheim Peninsula of Ellesmere Island (Northwest Territories, District of Franklin), *Geological Survey of Canada*,
1334 *Bulletin*, 529, 295–317, 2000.

1335 Mattson, M. D.: *Acid lakes and rivers*. In: *Environmental Geology*, Springer Netherlands, Dordrecht, 1999.

1336 McAndrews, J. H., Berti, A. A., and Norris, G.: *Key to the Quaternary pollen and spores of the Great Lakes region*,
1337 1973. 1973.

1338 Miller, G. H., Alley, R. B., Brigham-Grette, J., Fitzpatrick, J. J., Polyak, L., Serreze, M. C., and White, J. W. C.: Arctic
1339 amplification: can the past constrain the future?, *Quaternary Science Reviews*, 29, 1779–1790, 2010.

Deleted: Leavitt, S. W. and Danzer, S. R.: Method for batch processing small wood samples to holocellulose for stable-carbon isotope analysis, *Analytical Chemistry*, 65, 87–89, 1993.

Deleted: Martinez-Boti, M. A., Foster, G. L., Chalk, T. B., Rohling, E. J., Sexton, P. F., Lunt, D. J., Pancost, R. D., Badger, M. P. S., and Schmidt, D. N.: Plio-Pleistocene climate sensitivity evaluated using high-resolution CO_2 records, *Nature*, 518, 49–54, 2015.

Deleted: Ménot, G. and Burns, S. J.: Carbon isotopes in ombrogenic peat bog plants as climatic indicators: calibration from an altitudinal transect in Switzerland, *Organic Geochemistry*, 32, 233–245, 2001.

1352 Mitchell, W. T., Rybczynski, N., Schröder-Adams, C., Hamilton, P. B., Smith, R., and Douglas, M.: Stratigraphic and
1353 Paleoenvironmental Reconstruction of a Mid-Pliocene Fossil Site in the High Arctic (Ellesmere Island, Nunavut):
1354 Evidence of an Ancient Peatland with Beaver Activity, *Arctic*, 69, 185–204, 2016.

1355 Moore, P. D., Webb, J. A., and Collison, M. E.: Pollen analysis, Blackwell Scientific Publications, Oxford, 1991.

1356 Naafs, B., Inglis, G., Zheng, Y., Amesbury, M., Biester, H., Bindler, R., Blewett, J., Burrows, M., del Castillo Torres,
1357 D., and Chambers, F. M.: Introducing global peat-specific temperature and pH calibrations based on brGDGT bacterial
1358 lipids, *Geochimica et Cosmochimica Acta*, 208, 285–301, 2017.

1359 Niemann, H., Stadnitskaia, A., Wirth, S., Gilli, A., Anselmetti, F., Sinninghe Damsté, J., Schouten, S., Hopmans, E.,
1360 and Lehmann, M.: Bacterial GDGTs in Holocene sediments and catchment soils of a high Alpine lake: application of
1361 the MBT/CBT-paleothermometer, *Climate of the Past*, 8, 889–906, 2012.

1362 Niklasson, M. and Drakenberg, B.: A 600-year tree-ring fire history from Norra Kivills National Park, southern
1363 Sweden: implications for conservation strategies in the hemiboreal zone, *Biological Conservation*, 101, 63–71, 2001.

1364 Niklasson, M. and Granström, A.: Fire in Sweden – History, Research, Prescribed Burning and Forest Certification,
1365 *International Forest Fire News*, 30, 80–83, 2004.

1366 Niklasson, M. and Granström, A.: Numbers and sizes of fires: Long-term spatially explicit fire history in a Swedish
1367 boreal landscape, *Ecology*, 81, 1484–1499, 2000.

1368 Otto-Bliesner, B. L. and Upchurch Jr, G. R.: Vegetation-induced warming of high-latitude regions during the Late
1369 Cretaceous period, *Nature*, 385, 804, 1997.

1370 Pagani, M., Liu, Z., LaRiviere, J., and Ravelo, A. C.: High Earth-system climate sensitivity determined from Pliocene
1371 carbon dioxide concentrations, *Nature Geoscience*, 3, 27–30, 2010.

1372 Pearson, E. J., Juggins, S., Talbot, H. M., Weckström, J., Rosén, P., Ryves, D. B., Roberts, S. J., and Schmidt, R.: A
1373 lacustrine GDGT-temperature calibration from the Scandinavian Arctic to Antarctic: Renewed potential for the
1374 application of GDGT-paleothermometry in lakes, *Geochimica et Cosmochimica Acta*, 75, 6225–6238, 2011.

1375 Peterse, F., Prins, M. A., Beets, C. J., Troelstra, S. R., Zheng, H., Gu, Z., Schouten, S., and Sinninghe Damsté, J. S.:
1376 Decoupled warming and monsoon precipitation in East Asia over the last deglaciation, *Earth and Planetary Science
1377 Letters*, 301, 256–264, 2011.

1378 Powers, L. A., Werne, J. P., Johnson, T. C., Hopmans, E. C., Sinninghe Damsté, J. S., and Schouten, S.: Crenarchaeotal
1379 membrane lipids in lake sediments: A new paleotemperature proxy for continental paleoclimate reconstruction?,
1380 *Geology*, 32, 613–616, 2004.

1381 R Core Team: R: A language and environment for statistical computing. R Foundation for Statistical Computing,
1382 Vienna, Austria, 2016.

1383 Racine, C. H., Johnson, L. A., and Viereck, L. A.: Patterns of Vegetation Recovery after Tundra Fires in Northwestern
1384 Alaska, U.S.A, *Arctic and Alpine Research*, 19, 461–469, 1987.

1385 Robinson, M. M.: New Quantitative Evidence of Extreme Warmth in the Pliocene Arctic, *Stratigraphy*, 6, 265–275,
1386 2009.

1387 Rogers, B. M., Soja, A. J., Goulden, M. L., and Randerson, J. T.: Influence of tree species on continental differences
1388 in boreal fires and climate feedbacks, *Nature Geoscience*, 8, 228–234, 2015.

Deleted: Ravelo, A. C., Andreassen, D. H., Lyle, M., Lyle, A. O., and Wara, M. W.: Regional climate shifts caused by gradual global cooling in the Pliocene epoch, *Nature*, 429, 263–267, 2004.[†]
Raymo, M. E., Lisiecki, L. E., and Nisancioglu, K. H.: Plio-Pleistocene ice volume, Antarctic climate, and the global $\delta^{18}\text{O}$ record, *Science*, 313, 492–495, 2006.[†]

1395 Royer, D. L., Berner, R. A., and Park, J.: Climate sensitivity constrained by CO₂ concentrations over the past 420
1396 million years, *Nature*, 446, 530-532, 2007.

1397 Russell, J. M., Hopmans, E. C., Loomis, S. E., Liang, J., and Sinninghe Damsté, J. S.: Distributions of 5- and 6-methyl
1398 branched glycerol dialkyl glycerol tetraethers (brGDGTs) in East African lake sediment: Effects of temperature, pH,
1399 and new lacustrine paleotemperature calibrations, *Geochimica et Cosmochimica Acta*, 117, 56–69, 2018.

1400 Ryan, K. C.: Dynamic interactions between forest structure and fire behavior in boreal ecosystems, *Silva Fennica*, 36,
1401 13–39, 2002.

1402 Rybczynski, N., Gosse, J. C., Richard Harington, C., Wogelius, R. A., Hidy, A. J., and Buckley, M.: Mid-Pliocene
1403 warm-period deposits in the High Arctic yield insight into camel evolution, *Nature Communications*, 4, 1–9, 2013.

1404 Salzmann, U., Dolan, A. M., Haywood, A. M., Chan, W.-L., Voss, J., Hill, D. J., Abe-Ouchi, A., Otto-Bliesner, B.,
1405 Bragg, F. J., and Chandler, M. A.: Challenges in quantifying Pliocene terrestrial warming revealed by data-model
1406 discord, *Nature Climate Change*, 3, 969, 2013.

1407 Salzmann, U., Haywood, A. M., Lunt, D., Valdes, P., and Hill, D.: A new global biome reconstruction and data-model
1408 comparison for the middle Pliocene, *Global Ecology and Biogeography*, 17, 432–447, 2008.

1409 Shellito, C. J., Lamarque, J.-F. o., and Sloan, L. C.: Early Eocene Arctic climate sensitivity to pCO₂ and basin
1410 geography, *Geophysical Research Letters*, 36, 2009.

1411 Sinninghe Damsté, J. S.: Spatial heterogeneity of sources of branched tetraethers in shelf systems: The geochemistry
1412 of tetraethers in the Berau River delta (Kalimantan, Indonesia), *Geochimica et Cosmochimica Acta*, 186, 13–31, 2016.

1413 Sinninghe Damsté J.S., Rijpstra W.I.C., Foesel B.U., Huber K., Overmann J., Nakagawa S., Joong Jae Kim, Dunfield
1414 P.F. Dedysh S.N., Villanueva L. (2018) An overview of the occurrence of ether- and ester-linked iso-diabolic acid
1415 membrane lipids in microbial cultures of the Acidobacteria: Implications for brGDGT palaeoproxies for temperature
1416 and pH. *Organic Geochemistry*, 124, 63–76.

1417 Sinninghe Damsté, J. S., Rijpstra, W. I. C., Hopmans, E. C., Foesel, B. U., Wüst, P. K., Overmann, J., Tank, M.,
1418 Bryant, D. A., Dunfield, P. F., Houghton, K., and Stott, M. B.: Ether- and Ester-Bound iso-Diabolic Acid and Other
1419 Lipids in Members of Acidobacteria Subdivision 4, *Applied and Environmental Microbiology*, 80, 5207–5218, 2014.

1420 Sinninghe Damsté, J. S., Rijpstra, W. I. C., Hopmans, E. C., Weijers, J. W., Foesel, B. U., Overmann, J., and Dedysh,
1421 S. N.: 13, 16-Dimethyl octacosanedioic acid (iso-diabolic acid), a common membrane-spanning lipid of Acidobacteria
1422 subdivisions 1 and 3, *Applied and Environmental Microbiology*, 77, 4147–4154, 2011.

1423 Stap, L. B., de Boer, B., Ziegler, M., Bintanja, R., Lourens, L. J., and van de Wal, R. S.: CO₂ over the past 5 million
1424 years: Continuous simulation and new δ¹¹B-based proxy data, *Earth and Planetary Science Letters*, 439, 1–10, 2016.

1425 Swann, A. L., Fung, I. Y., Levis, S., Bonan, G. B., and Doney, S. C.: Changes in Arctic vegetation amplify high-
1426 latitude warming through the greenhouse effect, *Proceedings of the National Academy of Sciences of the United States*
1427 *of America*, 107, 1295-1300, 2010.

1428 Tedford, R. H. and Harington, C. R.: An Arctic mammal fauna from the early Pliocene of North America, *Nature*,
1429 425, 388–390, 2003.

1430 Van Wagner, C. E., Finney, M. A., and Heathcote, M.: Historical fire cycles in the Canadian Rocky Mountain parks,
1431 *Forest Science*, 52, 704-717, 2006.

Deleted: Rovere, A., Raymo, M. E., Mitrovica, J. X., Hearty, P. J., O'Leary, M. J., and Inglis, J. D.: The Mid-Pliocene sea-level conundrum: Glacial isostasy, eustasy and dynamic topography, *Earth and Planetary Science Letters*, 387, 27–33, 2014.†

Royer, D. L.: CO₂-forced climate thresholds during the Phanerozoic, *Geochimica et Cosmochimica Acta*, 70, 5665-5675, 2006.†

Deleted: Royles, J., Horwath, A. B., and Griffiths, H.: Interpreting bryophyte stable carbon isotope composition: Plants as temporal and spatial climate recorders, *Geochemistry, Geophysics, Geosystems*, 15, 1462–1475, 2014.†

Deleted: Schlesinger, W. H. and Vengosh, A.: Global boron cycle in the Anthropocene, *Global Biogeochemical Cycles*, 30, 219–230, 2016.†

Seki, O., Foster, G. L., Schmidt, D. N., Mackensen, A., Kawamura, K., and Pancost, R. D.: Alkenone and boron-based Pliocene pCO₂ records, *Earth and Planetary Science Letters*, 292, 201–211, 2010.†

Deleted: Skrzypek, G., Kałużny, A., Wojtuń, B., and Jędrysek, M.-O.: The carbon stable isotopic composition of mosses: A record of temperature variation, *Organic Geochemistry*, 38, 1770–1781, 2007.†

Deleted: Tripati, A. K., Roberts, C. D., and Eagle, R. A.: Coupling of CO₂ and Ice Sheet Stability over Major Climate Transitions of the Last 20 Million Years, *Science*, 326, 1394–1397, 2009.†

1454 Wang, X., Ryczynski, N., Harington, C. R., White, S. C., and Tedford, R. H.: A basal ursine bear (*Protarctos*
1455 *abstrusus*) from the Pliocene High Arctic reveals Eurasian affinities and a diet rich in fermentable sugars, *Scientific*
1456 *reports*, 7, 17722, 2017.

1457 Warden, L., Jung-Hyun, K., Zell, C., Vis, G.-J., de Stigter, H., Bonnín, J., and Sinninghe Damsté, J. S.: Examining
1458 the provenance of branched GDGTs in the Tagus River drainage basin and its outflow into the Atlantic Ocean over
1459 the Holocene to determine their usefulness for paleoclimate applications, *Biogeosciences*, 13, 5719, 2016.

1460 Weijers, J. W., Schefuß, E., Schouten, S., and Sinninghe Damsté, J. S.: Coupled thermal and hydrological evolution
1461 of tropical Africa over the last deglaciation, *Science*, 315, 1701–1704, 2007a.

1462 Weijers, J. W., Schouten, S., van den Donker, J. C., Hopmans, E. C., and Sinninghe Damsté, J. S.: Environmental
1463 controls on bacterial tetraether membrane lipid distribution in soils, *Geochimica et Cosmochimica Acta*, 71, 703–713,
1464 2007b.

1465 Weijers, J. W. H., Schouten, S., van den Donker, J. C., Hopmans, E. C., and Sinninghe Damsté, J. S.: Environmental
1466 controls on bacterial tetraether membrane lipid distribution in soils, *Geochimica et Cosmochimica Acta*, 71, 703–713,
1467 2007c.

1468 Whitman, E., Batllori, E., Parisien, M. A., Miller, C., Coop, J. D., Krawchuk, M. A., Chong, G. W., and Haire, S. L.:
1469 The climate space of fire regimes in north-western North America, *Journal of Biogeography*, 42, 1736–1749, 2015.

1470 Wright, C. S. and Agee, J. K.: Fire and vegetation history in the eastern Cascade Mountains, Washington, *Ecological*
1471 *Applications*, 14, 443–459, 2004.

1472 Yang, G., Zhang, C. L., Xie, S., Chen, Z., Gao, M., Ge, Z., and Yang, Z.: Microbial glycerol dialkyl glycerol tetraethers
1473 from river water and soil near the Three Gorges Dam on the Yangtze River, *Organic Geochemistry*, 56, 40–50, 2013.

1474 Yarie, J.: Forest fire cycles and life tables: a case study from interior Alaska, *Canadian Journal of Forest Research*,
1475 11, 554–562, 1981.

1476 Young, A. M., Higuera, P. E., Duffy, P. A., and Hu, F. S.: Climatic thresholds shape northern high-latitude fire regimes
1477 and imply vulnerability to future climate change, *Ecography*, 40, 606–617, 2017.

1478 Zech, R., Gao, L., Tarozo, R., and Huang, Y.: Branched glycerol dialkyl glycerol tetraethers in Pleistocene loess-
1479 paleosol sequences: three case studies, *Organic geochemistry*, 53, 38–44, 2012.

1480 Zell, C., Kim, J.-H., Moreira-Turcq, P., Abril, G., Hopmans, E. C., Bonnet, M.-P., Sobrinho, R. L., and Sinninghe
1481 Damsté, J. S.: Disentangling the origins of branched tetraether lipids and crenarchaeol in the lower Amazon River:
1482 Implications for GDGT-based proxies, *Limnology and Oceanography*, 58, 343–353, 2013.

1483 Zhu, C., Weijers, J. W., Wagner, T., Pan, J.-M., Chen, J.-F., and Pancost, R. D.: Sources and distributions of tetraether
1484 lipids in surface sediments across a large river-dominated continental margin, *Organic Geochemistry*, 42, 376–386,
1485 2011.

1486 Zink, K.-G., Vandergoes, M. J., Mangelsdorf, K., Dieffenbacher-Krall, A. C., and Schwark, L.: Application of
1487 bacterial glycerol dialkyl glycerol tetraethers (GDGTs) to develop modern and past temperature estimates from New
1488 Zealand lakes, *Organic Geochemistry*, 41, 1060–1066, 2010.

1489

Deleted: Waite, M. and Sack, L.: Shifts in bryophyte carbon isotope ratio across an elevation × soil age matrix on Mauna Loa, Hawaii: do bryophytes behave like vascular plants?, *Oecologia*, 166, 11–22, 2011.¶

Deleted: White, J., Ciais, P., Figge, R., Kenny, R., and Markgraf, V.: A high-resolution record of atmospheric CO₂ content from carbon isotopes in peat, *Nature*, 367, 153–156, 1994.¶

1497
1498

Table 1. Modern and recent Holocene fire return interval reconstructions for the candidate analogous regions considered in this study.

Region	Modern	Reference	Recent Holocene	Reference		
Alaskan Tundra	Seward Peninsula	273*	Up-Valley	263	Higuera et al. (2011)	
	Nulato Hills	306*				Down-valley
Alaskan Boreal	Porcupine/Upper Yukon (Central)	~100				
	Sites near Fairbanks, and Delta Junction (Central)	70130				
	Kenai Peninsula		Lynch et al. (2002)	Interior Alaska and Kenai Peninsula	198 ± 90	Lynch et al. (2002)
	Yukon river Lowlands	120	Kasischke et al. (2002)	Brooks Range	145	Higuera et al. (2009)
	Kuskokwim Mountains	218				
	Yukon-Tanama Uplands	330				
	Tanana-Kuskokwim Lowlands	178				
	Kobuk Ridges and Valleys	175				
	Davidson Mountains	403				
	North Ogilive Mountains	112				
	Ray Mountains	109				
	Yukon-Old Crow Basin	81				

Western North America	Darkwoods, British Columbia	~69	Greene and Daniels (2017)			
	Cascade Mountains, Washington	~27	Wright and Agee (2004)			
	Desolation Peak, Washington Coastal type	108-137				
	Desolation Peak, Washington Interior type	~52				
Eastern North America	Quebec – west	~270*	Bouchard et al. (2008)	Maine	≥ 800	Lorimer (1977)
	Quebec – east	>500*				
				Quebec – “Spruce zone”	570	de Lafontaine and Payette (2011)
				Quebec – “Fir zone”	>1000	
	Quebec – Abitibi northwest	418*	Bergeron et al. (2006 post-1940)^	Quebec – Abitibi northwest	189	Bergeron et al. (2006 post-1940)^
	Quebec – Abitibi southwest	388*		Quebec – Abitibi southwest	165	
	Quebec – Abitibi east	418*		Quebec – Abitibi east	141	
	Quebec – Abitibi southeast	2083*		Quebec – Abitibi southeast	257	
Quebec – Temiscamingue north	2083*	Quebec – Temiscamingue north		220		

	Quebec – Temiscamingue south	2777*		Quebec – Temiscamingue south	313	
	Quebec – Waswanipi	418*		Quebec – Waswanipi	128	
	Quebec – Central Quebec	388*		Quebec – Central Quebec	150	
	Quebec – North Shore	645*		Quebec – North Shore	281	
	Quebec – Gaspésia	488*		Quebec – Gaspésia	161	
	Quebec – northwestern lakeshore	99 [†]	Bergeron (1991)	Quebec – northwestern lakeshore	63 [†]	Bergeron (1991)
	Quebec – northwestern lake island	112 [†]		Quebec – northwestern – lake island	74 [†]	
Fennoscandia	Sweden	*	Niklasson and Drakenberg (2001); Niklasson and Granström (2004)	North Sweden	50-150	Niklasson and Granström (2004); Niklasson and Granström (2000)
				Southern Sweden	20	
	Central Sweden	*	Brown and Giesecke (2014)	Central Sweden - Klotjärnen	180	Brown and Giesecke (2014)
			Central Sweden - Holtjärnen	240		
Siberian Plateau	Northern	300	Kharuk et al. (2016); Kharuk et al. (2011)			
	Southern	80				
	Mean (64-71°N)	110				

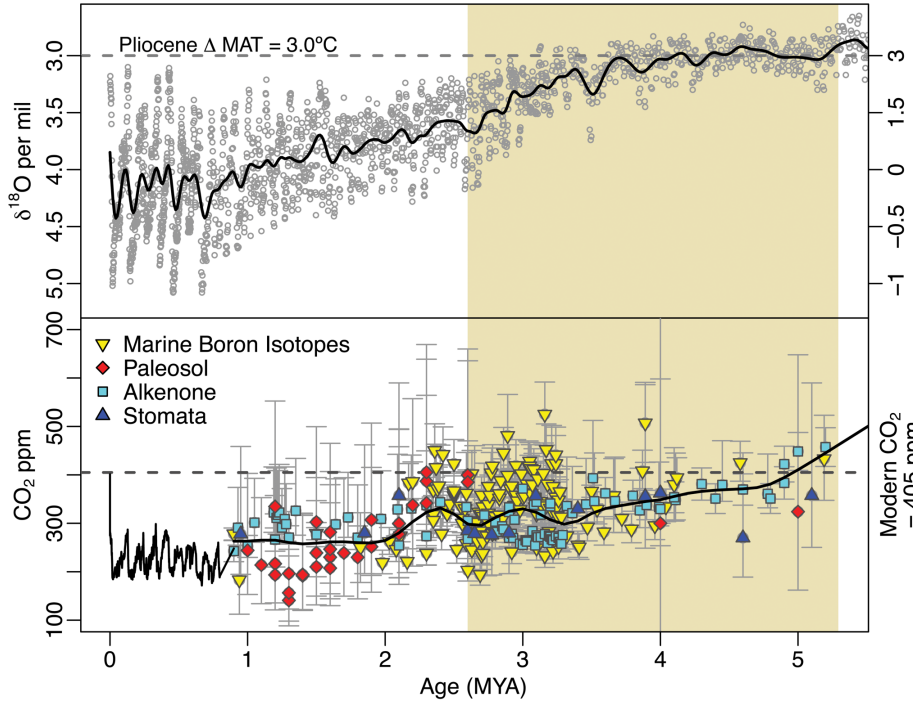
1499 [^] = The reciprocal converted from burn rate (%) (see Van Wagner et al., 2006)

1500 * = Estimates likely effected in some areas by human activity. In such instances Recent Holocene is preferred.

1501 [†] = Fire cycle

1502 [†] = 'Recent' here refers to records that (or have distinct sections that) begin after the end of the Holocene Climate

1503 Optima and end near present



1505

1506

1507

1508

1509

1510

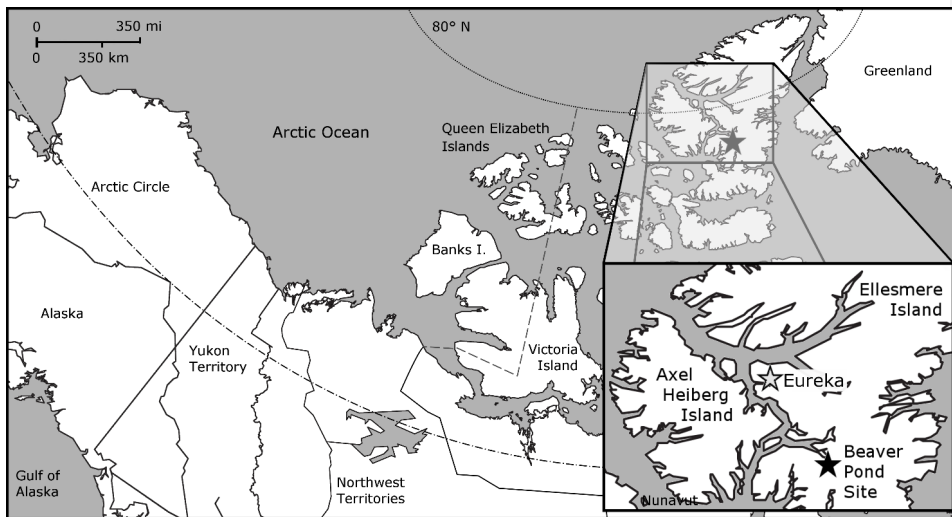
1511

1512

Figure 1: Global temperatures and atmospheric CO₂ concentration spanning the last 5 million years of Earth's history. Mean annual temperatures (MAT) are inferred from compiled δ¹⁸O foraminifera data (Lisiecki and Raymo, 2005) and plotted as anomalies from present (top panel). Modern atmospheric CO₂ measurements (NOAA/ESRL), and ice core observations from EPICA (Luthi et al., 2008) are compared with proxy estimates (bottom panel; see Table S1) for the Pliocene Epoch indicated with beige shading. Smoothed curves have been fit to highlight trends in pCO₂ and temperature during the Pliocene.

Deleted: The results from this paper (BP) are included with both age and pCO₂ error.

1515

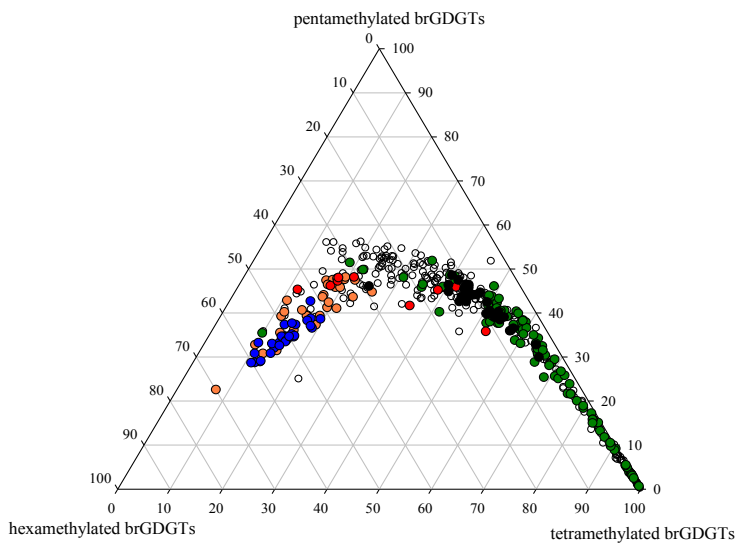


1516

1517 **Figure 2. Map of the Canadian Arctic Archipelago, highlighting the location of the Beaver Pond Site (Black**
1518 **Star; 78° 33' N; 82° 25' W) and Eureka Climate Station (Grey Star; 80° 13' N, 86° 11' W – used for modern**
1519 **climate comparison) on west-central Ellesmere Island.**

1520

- Global soil data set (De Jonge et al., 2014)
- Peat data set (Naafs et al., 2017)
- Lake sediments <10°C (Russell et al., 2018)
- Lake sediments 10–20°C (Russell et al. 2018)
- Lake sediments >20°C (Russell et al., 2018)
- Beaver Pond sediments (this study)



521
522
523
524
525
526
527
528

Figure 3. A ternary plot illustrating the fractional abundances of the tetra- (Ia-c), penta (IIa-c and II'a-c), and hexamethylated (IIIa-c and III'a-c) brGDGTs. The global soil dataset (open circles; De Jonge et al., 2014), the global peat samples (green circles; Naafs et al., 2017), and lake sediments from East Africa (black circles designate samples from lakes >20°C, red circles indicate samples from lakes between 10–20°C and orange circles designate samples from lakes <10°C; Russell et al., 2018) are included for comparison with the Beaver Pond sediments (blue circles; this study).

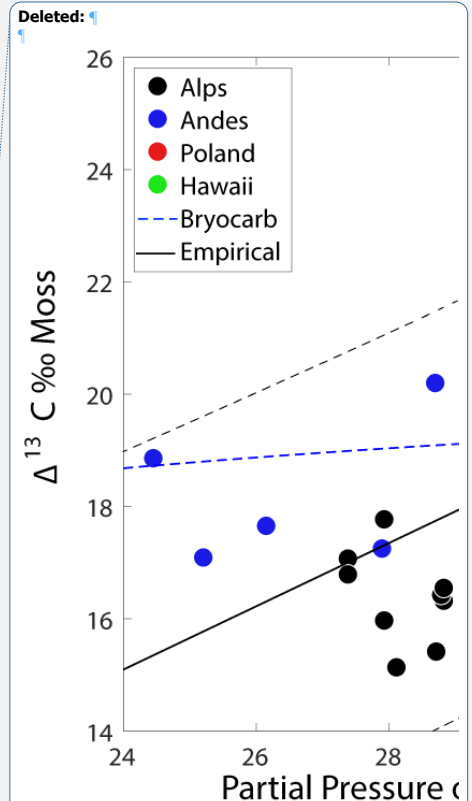
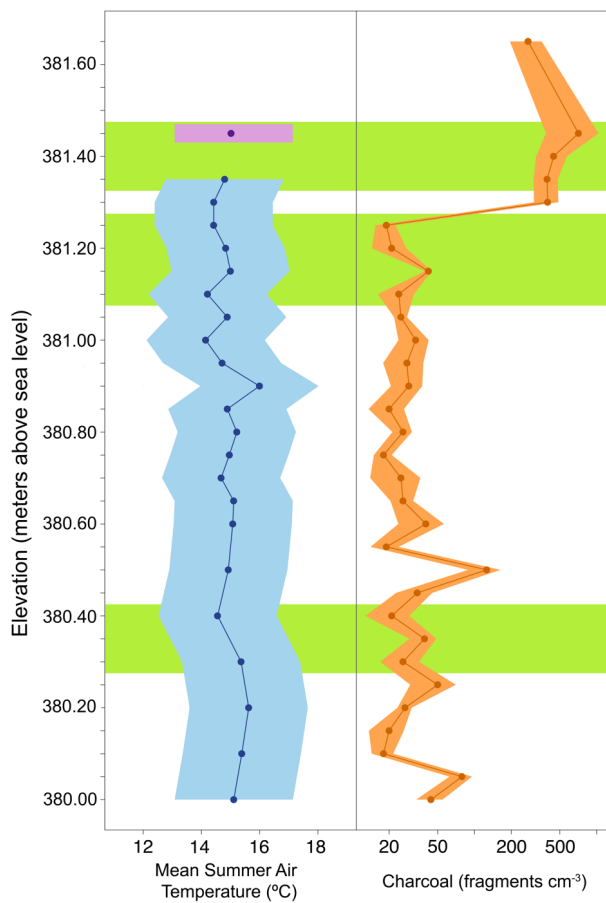


Figure 3. Sensitivity of carbon isotopic discrimination to the partial pressure of atmospheric CO₂ in mosses sampled from different elevational transects. Moss carbon isotope data collected from an elevational transects in the Swiss Alps (black dots; Ménot and Burns, 2001), the Peruvian Andes (blue dots; Royles et al., 2014), the mountains of Poland (red dots; Skrzypek et al. 2007), and Hawaii (green dots; Waite and Sack 2011). Partial pressure of atmospheric CO₂ calculated from atmospheric surface pressure reanalysis data (Dee et al., 2011) combined with atmospheric CO₂ observations from year moss samples were collected. All carbon isotopic measurements of mosses have been normalized to cellulose based on published regression of cellulose and whole moss values (Ménot and Burns, 2001) and reported as discrimination (Δ) from atmospheric δ¹³CO₂ (GlobalView-CO₂, 2013) from the year mosses were collected in units of ‰. Empirical model fit (black line) is plotted with prediction intervals (black dashed) compared with predictions from the BRYOCARB model (blue dashed; Fletcher et al. 2008) with parameters optimized to match observations.

Page Break: ... [4]

Formatted: Line spacing: Multiple 1.15 li
Deleted: 5



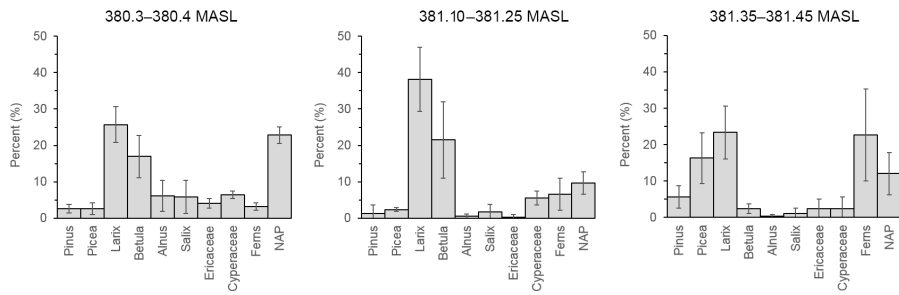
553

554 **Figure 4. Reconstruction of mean summer temperature and fire for the Canadian High Arctic during the**
 555 **Pliocene. Mean summer air temperature reconstructed from a brGDGT based proxy (blue; $\pm 2 \sigma$) and relative**
 556 **2010 data point in approximate relative position (purple; $\pm 2 \sigma$). Charcoal counts reported as the number of**
 557 **fragments per volume (fragments cm^{-3}) of peat (Orange $\pm 2 \sigma$). Green boxes indicate relative depths of pollen**
 558 **sampling. Elevation of the deposit is reported as meters above sea level. (Data: Table S3)**

Formatted: Caption, Line spacing: Multiple 1.15 li

1559
1560
1561

(A)



1562

1563

(B)

1564

1565

1566

1567

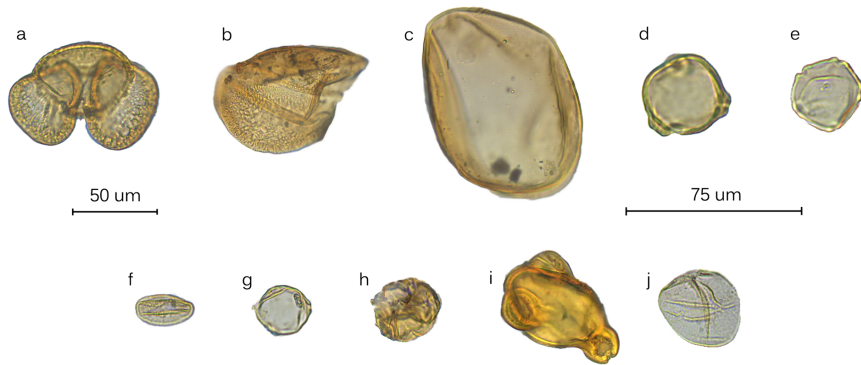
1568

1569

1570

1571

1572



1573

1574

1575

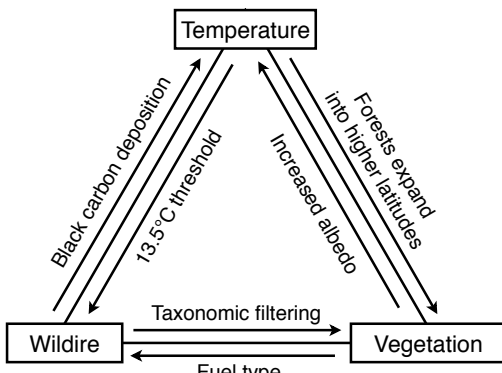
1576

1577

Figure 5. (A) Bar charts showing the relative pollen abundance in each portion of the section (error bars = 95% confidence intervals; MASL- Meters Above Sea Level). (B). Pollen plate of select grains encountered in the BP section: (a) *Pinus*, (b) half a *Picea* grain, (c) *Larix*, (d) *Betula*, (e) *Alnus*, (f) *Salix*, (g) *Myrica*, (h) ericaceous grain, (i) *Epilobium*, and (j) *Cyperaceae*. 50um scale = (a-c), 75um scale = (d-j).

Formatted: Line spacing: Multiple 1.15 li

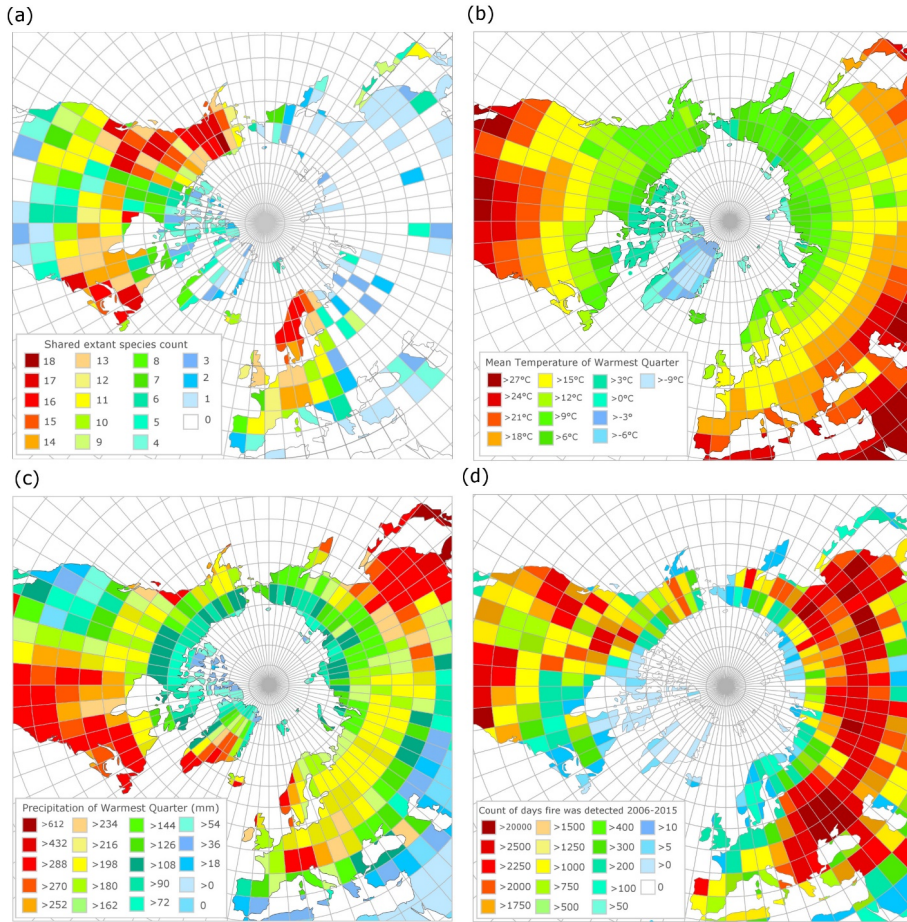
Deleted: 6



579
580

Figure 6: Examples of the feedbacks between temperature, vegetation and wildfire at the Beaver Pond site

- Formatted: Font: Bold
- Formatted: Font: Bold
- Formatted: Font: Bold



1582 **Figure 7.** (a) Modern geographic distribution of observed occurrences of species common to the Beaver Pond
 1583 species list, (b) Mean temperature of the warmest quarter (summer average) derived from WorldClim, (c)
 1584 Mean precipitation of the warmest quarter (summer rain) derived from WorldClim, (d) Count of unique fire
 1585 pixels detected per day, over 10 years from MODIS 6 Fire Product, normalized by area of the latitude by
 1586 longitude grid.

Formatted: Line spacing: Multiple 1.15 li
 Deleted: 7